

Summer 8-2019

# 3-Hydroxy Fatty Acids Induce Retinal Pigment Epithelial Cell Lipoapoptosis

Mona Hadidi

University of Nebraska - Lincoln, mona.hadidi1@gmail.com

Follow this and additional works at: <https://digitalcommons.unl.edu/nutritiondiss>



Part of the [Nutrition Commons](#)

---

Hadidi, Mona, "3-Hydroxy Fatty Acids Induce Retinal Pigment Epithelial Cell Lipoapoptosis" (2019). *Nutrition & Health Sciences Dissertations & Theses*. 83.

<https://digitalcommons.unl.edu/nutritiondiss/83>

This Article is brought to you for free and open access by the Nutrition and Health Sciences, Department of at DigitalCommons@University of Nebraska - Lincoln. It has been accepted for inclusion in Nutrition & Health Sciences Dissertations & Theses by an authorized administrator of DigitalCommons@University of Nebraska - Lincoln.

**3-HYDROXY FATTY ACIDS INDUCE RETINAL PIGMENT EPITHELIAL  
CELL LIPOAPOPTOSIS**

By

Mona Kassem Hadidi

A THESIS

Presented to the Faculty of  
The Graduate College at the University of Nebraska  
In Partial Fulfillment of Requirements  
For the Degree of Master of Science

Major: Nutrition

Under the Supervision of Professor Sathish Kumar Natarajan

Lincoln, Nebraska  
August, 2019

# 3-HYDROXY FATTY ACIDS INDUCE RETINAL PIGMENT EPITHELIAL CELL LIPOAPOPTOSIS

Mona Kassem Hadidi M.S.

University of Nebraska, 2019

Advisor: Sathish Kumar Natarajan

Mitochondrial fatty acid oxidation (FAO) plays an important role in maintaining metabolic homeostasis, especially during catabolic stress. Genetic mutation in gene that encodes for mitochondrial FAO enzymes could result in metabolic stress especially during fasting or hypoglycemic condition. Mutation in the active site residue (1528G>C) of long chain 3-hydroxy acyl CoA dehydrogenase (LCHAD) results in the loss of LCHAD enzyme activity. Children's with LCHAD mutation were known to accumulate 3-hydroxy fatty acids such as 3-hydroxy palmitic acid and 3-hydroxy myristic acids, long chain free fatty acids, acyl carnitine and 3-hydroxy dicarboxylic acid due to their defective enzyme activity. These accumulated 3-hydroxy fatty acids and long chain free fatty acids are toxic compound to the cellular tissues and results in the development of retinopathy. Here we hypothesize that increased levels of 3-hydroxy fatty acid due to a mutation in LCHAD would induce retinal pigment epithelial cell lipoapoptosis and palmitoleate (PO) protects against 3-hydroxy fatty acid-induced retinal lipoapoptosis. Normal human immortalized retinal pigment epithelial cells (ARPE-19) were treated with 3-hydroxy fatty acid (3-HFA)

for 24 hours and biochemical markers of lipoapoptosis such as characteristic nuclear morphological changes of apoptosis and caspase 3/7 activity were measured. Mitochondrial bioenergetics were assessed using Seahorse XF24 extracellular flux analyzer and lipid droplets were stained with oil red 'O' dye. After 24-hours of 3-HFAs treatment to ARPE-19 cells, we observed a significant increase in percent apoptotic nuclei and caspase 3/7 activity compared to the vehicle treated cells suggesting retinal lipoapoptosis. Further, percent cell survival and metabolic activity were decreased in cells treated with 3-HFA compared to vehicle treatment. 3-HFA-induced retinal cell lipoapoptosis is cJun N-terminal kinase- and caspase-dependent lipoapoptosis. Treatment of 3-HFAs to retinal cells showed decreased mitochondrial bioenergetics as evidenced by a decrease in basal respiration, ATP production, maximal respiration and mitochondrial coupling efficiency compared to vehicle ( $p < .05$ ). We also observed that PO protects against 3-HFA-induced retinal lipoapoptosis. However further investigations are required to understand the mechanism of palmitoleate protection. In conclusion, 3-HFAs induce lipid droplet accumulation and mitochondrial stress resulting in retinal pigment epithelial cell lipoapoptosis, which was protected with PO supplementation.

**Dedication**

This thesis is dedicated to my family, especially my parents, Kassem and Barqiah, my husband, Haitham, and my daughters, Seba and Dema.

## List of Abbreviations and Symbols

FAs	Fatty acids
FAO	Fatty acid oxidation
FAODs	Fatty acid oxidation disorders
MTP	Mitochondrial trifunctional protein
SCAD	Short-chain acyl-CoA dehydrogenase
MCAD	Medium-chain acyl-CoA dehydrogenase
LCHAD	Long-chain 3-hydroxy acyl-CoA dehydrogenase
VLCAD	Very long-chain acyl-CoA dehydrogenase
CPT-II	Carnitine palmitoyl transferase 2
LCHADD	Long-chain 3-hydroxy acyl-CoA dehydrogenase deficiency
DNA	Deoxyribonucleic acid
DRs	Death receptors
TNF	Tumor-necrosis factors
AIF	Apoptosis-inducing factor
ROS	Reactive oxygen species
ATP	Adenosine Triphosphate
OXPPOS	Oxidative phosphorylation
MPT	Mitochondrial permeability transition
HMG-CoA	Hydroxy-3-methylglutaryl-coenzyme-A
MAPK	Mitogen-activated protein kinase
FoxO3	Forkhead family of transcription factor class O3

3-HFA	3-Hydroxy fatty acid
3-HMA	3-Hydroxy myristic acid
3-HPA	3-Hydroxy palmitic acid
RPE	Retinal pigmented epithelium
CPT	Carnitine palmitoyl transferase
hiPSC	Human-induced pluripotent stem cell
MCFT	Medium chain fatty acids
PA	Palmitic acid
MA	Myristic acid
PO	Palmitoleic acid
SFA	Saturated free fatty acid
LDL	Low-density lipoprotein
HDL	High-density lipoprotein
DMEM	Dulbecco's Modified Eagle's Medium
FBS	Fetal bovine serum
BSA	Bovine serum albumin
PARP	Poly (ADP-ribose) polymerase
DAPI	4',6-diamidino-2-phenylindole
PUMA	p53 upregulated modulator of apoptosis
BORC	Biomedical and Obesity Research Core
OCR	Oxygen consumption rate
PBS	Phosphate buffered saline
NADH	Nicotinamide adenine dinucleotide

ECAR	Extracellular acidification rate
SEM	Standard error of Mean
ANOVA	Analysis of variance



## **Acknowledgements**

I would like to express my sincere appreciation to my advisor Dr. Sathish Kumar Natarajan for his support and guidance in conducting this research, I could not be more appreciative.

I also want to thank Dr. Seung-Hyun Ro and Dr. Jiujiu Yu for agreeing to serve on my supervisory committee. I am grateful for their mentorship in guiding this research.

I also would like to thank the staff in Biomedical and Obesity Research Core (BORC) facility for using their equipment for mitochondria stress and Dr. Chung facility in which I used the light microscope for my experiments.

I would also like to acknowledge my colleagues and lab mates Mr. Ezhumalai Muthukrishnan, Mr. Prakash Sahoo, Mrs. Philma-Glora Muthuraj, Mrs. Madison Kraus, Mrs. Jillian Power, and Mrs. Taylor Bruett for their help, cooperation, support, and most importantly friendship. Thanks to King Abdullah scholarship program (Saudi Arabia) for financially supporting my studies at UNL. Thanks for National Institute of Health, General Medical Sciences, and Nebraska Center for the Prevention of Obesity Disease, P20GM104320.

Finally, I owe my sincere gratitude and gratefulness to my family, especially my parents, Kassem Hadidi and Barqiah Al-Ardi, my husband, Haitham Hadidi, and daughters, Seba and Dema for their endless support and encouragement. Special thanks to my parents for the endless support and prayers and to husband and daughters for their support and patience that

enabled me to pursue my studies. I love you all. You stand behind me firmly, and together we have experienced many joyous moments and endured many stressful occasions. You are the light, source, and motivation for my dreams.

## Table of Contents

<b>DEDICATION .....</b>	<b>i</b>
<b>LIST OF ABBREVIATIONS AND SYMBOLS.....</b>	<b>ii</b>
<b>ACKNOWLEDGEMENTS .....</b>	<b>v</b>
<b>LIST OF TABLES .....</b>	<b>ix</b>
<b>LIST OF FIGURES.....</b>	<b>x</b>
<b>1. CHAPTER I: INTRODUCTION.....</b>	<b>1</b>
<b>1.1 Fatty Acid (FA) Metabolism .....</b>	<b>2</b>
<b>1.1.1 Mitochondrial Fatty Acid Oxidation.....</b>	<b>3</b>
<b>1.1.2 Fatty Acid Oxidation Disorders (FAODs).....</b>	<b>4</b>
<b>1.1.3 Long Chain 3-Hydroxy Acyl-CoA Dehydrogenase Deficiency (LCHAD) .....</b>	<b>5</b>
<b>1.2 Apoptosis.....</b>	<b>6</b>
<b>1.2.1 Extrinsic and Intrinsic Pathway of Apoptosis .....</b>	<b>8</b>
<b>1.3 Mitochondria.....</b>	<b>9</b>
<b>1.3.1 Mechanisms of Mitochondria in Inducing Pathophysiology.....</b>	<b>10</b>
<b>1.3.2 Role of Mitochondria in Fatty Acid Oxidation Disorders.....</b>	<b>12</b>
<b>1.4 Retinal Pigmented Epithelial Cells in LCHAD Deficiency .....</b>	<b>14</b>
<b>1.4.1 Apoptosis of Retinal Cells in LCHAD Deficiency .....</b>	<b>15</b>
<b>1.5 Dietary Supplementation as a Protective Strategy against LCHAD Deficiency .....</b>	<b>16</b>
<b>1.5.1 Medium Chain Fatty Acids (MCFA) Supplementation .....</b>	<b>16</b>
<b>1.5.2 Carnitine Supplementation .....</b>	<b>17</b>
<b>1.5.3 Docosahexaenoic acid (DHA) supplementation.....</b>	<b>17</b>
<b>1.5.4 Protection Role of Palmitoleate Supplementation .....</b>	<b>18</b>
<b>1.6 Central Hypothesis, Purpose, and Specific Aims.....</b>	<b>20</b>
<b>1.6.1 Central Hypothesis and Purpose.....</b>	<b>20</b>
<b>1.6.2 Specific Aims .....</b>	<b>21</b>
<b>2. CHAPTER II: MATERIALS AND METHODS.....</b>	<b>22</b>
<b>2.1 Cell Culture .....</b>	<b>22</b>
<b>2.1.1 Sub-culturing Cells .....</b>	<b>22</b>
<b>2.1.2 Counting Cells.....</b>	<b>22</b>
<b>2.1.3 Cell Seeding .....</b>	<b>23</b>
<b>2.2 Fatty Acids Preparations .....</b>	<b>23</b>
<b>2.2.1 Treatment of 3-Hydroxy Fatty Acids (3-HFA).....</b>	<b>24</b>
<b>2.3 Apoptotic Nuclear Morphological Changes .....</b>	<b>25</b>
<b>2.4 Measurements of Caspase 3/7 Activity .....</b>	<b>25</b>
<b>2.5 Mitochondrial Stress.....</b>	<b>26</b>
<b>2.5.1 Plating Cultures and Hydrating Sensor Cartridge .....</b>	<b>26</b>

2.5.2 Preparing Assay Medium .....	27
2.5.3 Preparing Stock Compounds.....	27
2.5.4 Running XF Assay and Measuring Oxygen Consumption Rate (OCR) .....	28
2.6 Western Blotting.....	28
2.6.1 Protein Isolation.....	28
2.6.2 Protein Estimation .....	28
2.6.3 Sodium Dodecyl Sulfate-Polyacrylamide Gel Electrophoresis (SDS-PAGE) Gel and Immunoblot Analysis .....	29
2.6.4 Immunoblot Detection .....	30
2.7 Oil Red O staining .....	30
2.8 Measuring Cell Survival Using 3-(4,5-dimethylthiazol-2-yl)-2,5- diphenyl tetrazolium bromide (MTT) Assay .....	31
2.9 Z-VAD and JNK inhibitors .....	31
2.10 Statistical Analysis.....	31
3. CHAPTER III: RESULTS .....	32
3.1 Results .....	32
3.1.1 Treatment of 3-Hydroxy Palmitic Acids (3-HPA) Decreased Mitochondrial Bioenergetics in Retinal Pigmented Epithelial Cells (ARPE-19) .....	32
3.1.2 3-Hydroxy Fatty Acids (3-HFAs) Induce Retinal Pigment Epithelial Cell (ARPE-19) Lipoapoptosis .....	35
3.1.3 Saturated Free Fatty Acids Palmitic Acid (PA) and Myristic Acid (MA) Did not Induce in ARPE-19 Lipoapoptosis .....	40
3.1.4 Biochemical Hallmark of Apoptosis.....	46
3.1.5 Palmitoleic Acid (PO) Protects Against 3-HFA-Induced Lipotoxicity.....	47
3.1.6 Retinal Cells Accumulated Lipid Droplet with 3-HPA or 3-HMA Treatment.....	50
3.1.7 3-HFA-Induces Retinal Cell Lipoapoptosis is c-Jun N-Terminal Kinase Activation.....	53
3.1.8 3-HFA Induces Retinal Cell Lipoapoptosis is Caspase Dependent.....	54
CHAPTER IV: DISCUSSION, CONCLUSION, AND FUTURE DIRECTIONS ...	58
4.1 Discussion:.....	58
4.2 Conclusions and Future Directions.....	65
REFERENCES .....	66

**List of Tables**

1.1	Comparison of Fatty Acids Oxidation Pathways .....	2
-----	--	---

## List of Figures

- Fig. 1. The extrinsic and intrinsic apoptotic pathways. At the plasma membrane, extrinsic pathway is activated when death receptors ligands bind to a subset of tumor necrosis factor receptor (TNF) receptors including TNFR1, Fas receptor, and death receptors. These receptors activate the procaspases 8 and 10 which leads to the activation of caspase 3 and 7 resulting in apoptosis. Intrinsic pathway is modulated by cell stressors such as Endoplasmic reticulum stress, DNA damage, nutritional stress and hypoxia. Mitochondrial outer membrane permeabilization (MOMP) occurs via the interaction of pro-apoptotic BH3 containing proteins such as BAX and BAK and BAX/BAK oligomerization. Pro-apoptotic intermembrane space (IMS) releases Cytochrome c (Cyt c) and second mitochondria-derived activator of caspase (SMAC) resulting in activating procaspase 9. Active caspase 9 cleaves pro-caspase 3 and 7 resulting in their activation for caspase-dependent apoptosis. This figure is adopted and modified from (Kalkavan & Douglas, 2017)..... 7
- Fig. 2. Mitochondrial dysfunction provoked by fatty acids and acyl carnitines accumulating in FAOD. In defective fatty acid oxidation (FAO) pathway, the acyl-CoA can't be converted into Acetyl-CoA resulting in higher accumulation of the substrates such as acyl carnitines and fatty acids. The accumulation of these compounds is toxic to the heart, liver, muscle, and brain tissue's that relay on fatty acids for energy. This lipotoxicity alters the mitochondrial bioenergetic functions and increases oxidative stress. This figure is adopted from (Wajner & Umpierrez, 2016) ..... 11
- Fig. 3. Schematic of (a) Hematocytometer and (b) counting chamber ..... 23
- Fig. 4. 24-well plate of a control and 3-HFA treated ARPE-19 cells..... 24
- Fig. 5. Schematic representation of SDS-PAGE gel and loading wells..... 29

- Fig. 6. Mitochondrial bioenergetics functions in ARPE-19 cells treated with 3-HPA. A) Oxygen consumption rate (OCR) for 100 minutes in vehicle and 3-HPA treated ARPE-19 cells. B) Basal respiration (B), Maximal respiration (C), ATP production (D), Coupling efficiency (E), Spare respiratory capacity (F) , and Proton Leak of ARPE-19 cells treated with 3-HPA and compared with vehicle ARPE-19 cells, respectively\* indicates P-value with different level of significance compared to vehicle treatment, \*(<0.05). \*\* (<0.01), and \*\*\*(<0.001). The data is represented mean  $\pm$  SEM from five independent experiments, n=5. The statistical significance of the observed differences were obtained by analysis of variance (ANOVA) and Tukey post-hoc test..... 33
- Fig. 7. Representative phase contrast and fluorescent DAPI stained live cell images of ARPE-19 cells with 3-HPA treatment. This representative figure shows that 3-hydroxy palmitic acids (3-HPA) induced nuclear morphological changes in retinal pigment epithelial cell (ARPE-19) lipoapoptosis. (A and B) are vehicle cells. (C-H) are ARPE-19 cells were treated with different concentrations of 3-HPA (100, 200, and 250  $\mu$ M). Scale bar represents 200  $\mu$ M..... 37
- Fig. 8. Representative phase contrast and fluorescent DAPI stained live cell images of ARPE-19 cells with 3-HMA treatment. This representative figure shows that 3-hydroxy myristic acids (3-HMA) nuclear morphological changes in in retinal pigment epithelial cell (ARPE-19) lipoapoptosis. (A and B) are vehicle cells. (C-H) are ARPE-19 cells were treated with different concentrations of 3-HMA (100, 200, and 250  $\mu$ M). Scale bar represents 200  $\mu$ M..... 38
- Fig. 9. Evidence for cell death in APRE-19 cells with 3-HFA treatment. A) Apoptotic nuclei percent for ARPE-10 cells treated with different concentrations of 3-hydroxy myristic acid (3-HMA) (100- 250  $\mu$ M) and B) Cells treated with 3-hydroxy palmitic acid (3-HPA) (100-250  $\mu$ M). C) Caspase 3/7 activity represented as fold change in ARPE-19 cells treated with 3-HMA D) cells treated with 3-HPA. E and F) Percent cell survival of ARPE-19 with different concentrations of 3-HMA or 3-HPA treatment. \* indicates P-value with different level of significance, \*(<0.05). \*\* (<0.01), and \*\*\*(<0.001). The differences in the apoptotic changes reached a statistical significance by obtaining that using ANOVA and Tukey test..... 40

- Fig.10 Representative Phase contrast and fluorescent DAPI stained live cell images of ARPE-19 cells with MA treatment. This representative figure shows that myristic acids (MA) did not increased staining of DAPI suggesting no change in characteristics of nuclear morphological changes in in retinal pigmented epithelial cell (ARPE-19) lipoapoptosis. (A and B) are vehicle cells. (C, D, E, F, G, H, I and J) ARPE-19 cells were treated with different concentrations of MA (100, 150, 200, and 250  $\mu$ M). Scale bar represents 200  $\mu$ M..... 42
- Fig.11 Representative Phase contrast and fluorescent DAPI stained live cell images of ARPE-19 cells with PA treatment. This representative image show that palmitic acids (PA) did not increase staining of DAPI suggesting no change in characteristics of nuclear morphological changes in in retinal pigment epithelial cell (ARPE-19) lipoapoptosis. (A and B) vehicle treated cells. (C, D, E, f, G, H, I and J) ARPE-19 cells were treated with different concentrations of PA (100, 150, 200, and 250  $\mu$ M). Scale bar represents 200  $\mu$ M..... 44
- Fig.12 Apoptotic nuclei percent for ARPE-10 cells treated with different concentrations of myristic acid (MA) (100-250  $\mu$ M) (A) and ARPE-19 cells treated with different concentrations of palmitic acid (PA) (100-250  $\mu$ M) (B). Caspase 3/7 activity in ARPE-19 cells treated with MA (C) and PA (D). \* indicates P-value with different level of significance, \*(<0.05). \*\* (<0.01), and \*\*\* (<0.001)..... 45
- Fig.13 Immunoblot analysis of Cleaved PARP, PUMA, Cleaved Caspase 3, and Actin in vehicle and 3-HPA/3-HMA treated ARPE-19 cells. Vehicle cells were isopropanol treatment and 3-HPA (250  $\mu$ M) or 3-HMA (250  $\mu$ M) treated cell lysates were analyzed after 12, 18, and 24 hours of treatment..... 47
- Fig.14 Apoptotic cell death and caspase activation in ARPE-19 cells treated with 3-HPA or 3-HMA along with palmitoleate. Apoptotic nuclei percent for ARPE-19 cells treated with 3-HMA and PO (A) and cells treated with 3-HPA and PO (B). Caspase 3/7 activation in ARPE-19 cells treated with 3-HMA and PO (C) and cells treated with 3-HPA and PO (D). Percent cell survival of ARPE-19 cells with 3-HMA (E) or 3-HPA (F) with and without palmitoleate (PO). Data represents mean  $\pm$  SEM from five independent experiments, n=5. \* indicates P-value with different level of significance of 3-HPA or 3-



HMA compared to vehicle, \*( $P < 0.05$ ). \*\* ( $P < 0.01$ ), and \*\*\*( $P < 0.001$ ). # $P > 0.05$  compared to 3-HPA or 3-HMA..... 49

Fig.15 Lipid droplet accumulation for ARPE-19 cells. Cells stained with Oil red 'O' assay visualized under light microscope. Control cells were treated with Vehicle (A) and Palmitoleate (B). Retinal cells with 250  $\mu\text{M}$  of 3-HMA (C) and 3-HPA treatment (E) for 24 hours showed increased Oil red 'O' staining. Co-treatment of palmitoleate (PO) with of 250  $\mu\text{M}$  3-HPA or 3-HMA (D and F) resulted in decreased Oil red 'O' staining. The images are representative images from three independent experiments,  $n=3$ . ..... 52

Fig.16 Oil red 'O' assay absorbance in ARPE-19 cells. ARPE-19 cells treated with only 3-HMA (250  $\mu\text{M}$ ) and both 3-HMA (250  $\mu\text{M}$ ) and PO (200  $\mu\text{M}$ ) (A). Cells treated with 3-HPA (250  $\mu\text{M}$ ) alone and co-treated with 3-HPA (250  $\mu\text{M}$ ) and PO (200  $\mu\text{M}$ ) (B). \* indicates P-value with different level of significance of 3-HPA or 3-HMA compared to vehicle, \*( $< 0.05$ ). \*\* ( $< 0.01$ ), and \*\*\*( $< 0.001$ ). # indicates P-value for 3-HPA or 3-HMA with PO compared to 3-HPA or 3-HPA ..... 53

Fig.17 Caspase 3/7 activity and percent cell survival in ARPE-19 cells treated with JNK-i. Caspase 3/7 activity were measured when cells were treated with 3-HMA and co-treated with 3 HMA and JNK inhibitor (SP600125, JNKi) (A) or treated with only 3-HPA or co-treated with 3-HPA and JNK-i. (B). Percent cell survival were measured when cells were treated with only 3-HMA or co-treated with 3-HMA JNKi (C) and only 3-HPA and co-treated with 3-HPA and JNKi (D). Data represent mean  $\pm$  SEM from five independent experiments,  $n=5$ . \*indicates P-value with different level of significance of 3-HPA or 3-HMA compared to vehicle (veh), \*( $< 0.05$ ). \*\* ( $< 0.01$ ), and \*\*\*( $< 0.001$ ). #  $P < 0.05$  compared to 3-HMA or 3-HPA treatment .....55

Fig.18 Caspase 3/7 activity and percent cell survival in ARPE-19 cells treated with Z-VAD. Caspase 3/7 activity were measured when cells were treated with 3-HMA and co-treated with 3 HMA and caspase inhibitor (Z-VAD fmk) (A) or treated with only 3-HPA or co-treated with 3-HPA and Z-VAD (B). Percent cell survival were measured when cells were treated with only 3-HMA or co-treated with 3-HMA Z-VAD (C) and only 3-HPA and co-treated with 3-HPA and Z-VAD (D). Data represent mean  $\pm$  SEM from five independent

experiments, n=5. \*indicates P-value with different level of significance of 3-HPA or 3-HMA compared to vehicle (veh), \*(<0.05). \*\* (<0.01), and \*\*\*(<0.001). # P<0.05 compared to 3-HMA or 3-HPA treatment .....56

## 1. CHAPTER I: INTRODUCTION

### 1.1 Fatty Acid (FA) Metabolism

Metabolism is the set of chemical reactions that occur within living cells in order to convert food into energy for the cellular processes (catabolism) and to convert small nutrients into larger molecules (anabolism). In living organisms, fatty acids (FAs) are essential components and building blocks for cellular membranes and provide energy for the body. Fat lipolysis is the biochemical process that takes place in the cytoplasm where the large fatty molecules such as triglycerides can be broken down and hydrolyze into glycerol and three molecules of fatty acids (FAs) in which enters mitochondria for its metabolism. The FAs are metabolized by three types fatty acid oxidation pathways such as mitochondrial- $\beta$  oxidation, microsomal  $\omega$ - oxidation and peroxisomal beta-oxidation, these pathways are different from each other and these differences are illustrated if **Table 1**. Mitochondrial  $\beta$ -oxidation is the most important pathway in living organisms which oxidizes the released FAs into two carbon units of acetyl CoA. Fatty acid oxidation (FAO) occurs with help of multiple enzymatic reactions. Translocation of fatty acids across the mitochondrial outer and inner membrane were carried out with the help of carnitine palmitoyl-transferase I and II (CPT I&II). Long-chain fatty acyl-carnitine enters the mitochondrial outer membrane by binding to carnitine via CPT-I and CPT-II translocase that transfer the fatty acyl-carnitine into the mitochondrial matrix, where Beta-oxidation pathway takes place. In this pathway, two carbons are cleaved from the long-chain acyl-CoA to

form acetyl-CoA by breaking the bond between beta carbon and gamma carbon. Thus, formed acetyl-CoA can enter tricarboxylic acid cycle in the mitochondrial matrix.

**Table 1 Comparison of Fatty Acids Oxidation Pathways**

	<b>Beta-Oxidation</b>	<b>Omega-Oxidation</b>	<b>Peroxisome-Oxidation</b>
<b>Location</b>	Mitochondrial matrix for all tissues except erythrocyte and adrenal medulla	Microsomes	Peroxisome
<b>Substrate</b>	Long, medium, short chain fatty acids	Long and very long fatty acids	Bile acids intermediates, very long fatty acids
<b>Benefits</b>	Major pathway to maintain mitochondrial homeostasis and production of ATP	Oxidation of omega carbon, when beta-oxidation defect, this pathway becomes active	Oxidation of the beta carbon of the fatty acyl CoA molecule
<b>Deficiencies</b>	HADHA deficiency Systemic carnitine deficiency, carnitine cycle disorder	-----	Zellweger syndrome X-linked adrenoleukodystrophy (X-ALD), Acyl-CoA oxidase deficiency (ACOX1) deficiency, diastolic blood pressure (DBP) deficiency

### **1.1.1 Mitochondrial Fatty Acid Oxidation**

Mitochondrial  $\beta$ -oxidation is the predominant FA oxidation pathway for cellular energy needs, plays an important role in maintaining metabolism homeostasis, especially during catabolic stress situations such as infection, disease, exercise, and fasting conditions. A large number of fatty acid oxidation disorders (FAODs) have been associated with a genetic defect in enzymes involved in fatty acid oxidation pathways (Wilcken, 2010). Mitochondrial trifunctional protein (MTP) is one of the complex enzymes that is required for the mitochondrial fatty acid oxidation (FAO). MTP is a multi-enzyme complex located in the mitochondrial inner membrane as a hetero-octamer and it contains four subunits: alpha-subunits and four beta-subunits. Alpha subunit contains enoyl-CoA hydratase and 3-hydroxyacyl-CoA dehydrogenase activity and beta subunit has 3-ketoacyl CoA thiolase activity. The oxidation involves four main enzymes and they are acyl-CoA dehydrogenase, enoyl-CoA hydratase and 3-hydroxyacyl-CoA dehydrogenase, and thiolase respectively. Any deficiency in one of these enzymes results in blockage of FAO process leading to fatty acids oxidation disorders. FAO is highly active in major metabolic organs like heart, liver and muscle cells and therefore FAO disorders that are associated with beta-oxidation are mostly expressed in the organs that rely on FAs metabolism predominantly affects liver, heart, and muscles (Wajner & Umpierrez, 2016).

### **1.1.2 Fatty Acid Oxidation Disorders (FAODs)**

FAODs are inherited metabolic diseases that are classified as inborn errors metabolism. FAODs are autosomal recessive genetic disorders which are caused as result of defects in genes that encodes mitochondrial FAO enzymes. The incidence of FAODs is about 1 in every 10,000 individuals (Merritt, Norris, & Kanungo, 2018). There are more than fifteen different FAODs, the most common disorders are short-chain acyl-CoA dehydrogenase (SCAD), medium-chain acyl-CoA dehydrogenase (MCAD), long-chain 3-hydroxy acyl-CoA dehydrogenase (LCHAD), and very long-chain acyl-CoA dehydrogenase (VLCAD) deficiency (Wajner & Umpierrez, 2016). The four most common enzyme deficiencies are carnitine palmitoyl transferase 2 (CPT-II), very long-chain acyl-CoA dehydrogenase (VLCAD), long-chain 3-hydroxyacyl-CoA dehydrogenase (LCHAD), and mitochondrial trifunctional protein (MTP). Individuals with FAOD accumulate toxic compounds in their circulations such as fatty acids and fatty acyl-carnitine. These disorders can be diagnosed in early stage of newborn life through laboratory analysis by measuring the levels of free fatty acids, dicarboxylic acid, and acyl-carnitine metabolites in blood and urine sample using Tandem Mass Spectrometry and Gas Chromatography (Enns et al., 2000).

Newborns who are diagnosed with FAOD usually have a multi-organ failure with a wide range of severity such as fatigue, hypoglycemia, rhabdomyolysis, hepatopathy, cardiomyopathy, and skeletal myopathy. These symptoms are mostly associated and worsened by fasting, infection, cold

exposure, exercise, infections, and other catabolic situations that require a high energy usage. Majority of the studies have indicated that the most associated reason for pathophysiology in FAODs is energy deficiency. Further, accumulating evidence that indicate the role of toxic fatty acids and fatty acyl carnitine metabolites in disturbing mitochondrial homeostasis which results in the development of most pathophysiology of FAODs (Wajner & Umpierrez, 2016).

### **1.1.3 Long Chain 3-Hydroxy Acyl-CoA Dehydrogenase Deficiency (LCHAD)**

Long-chain 3-hydroxy acyl-CoA dehydrogenase deficiency (LCHAD) is a disorder that is characterized by lack in LCHAD enzyme activity that is required for fatty acid  $\beta$ -oxidation in the mitochondria. The incidence of LCHAD mutation is 1:50,000 newborns (Hagenfeldt, Venizelos, & Von Döbeln, 1995). LCHAD is inherited disorder that has homozygous mutation in *HADHA* gene c.1528G>C affecting LCHAD enzyme activity (Padmini et al., 2015). As a result of this disorder, the body can't utilize long-chain fatty acids resulting in their accumulation as acyl-carnitine and long chain fatty acids in the systemic circulation.

Clinical presentations of LCHAD deficiency involves pathologies of the organs that relay on the mitochondria for energy supply including heart, muscle, liver, and eye. LCHAD deficient individuals usually present with common features; hypoglycemia, metabolic acidosis, skeletal myopathy, hypotonia, cardiomyopathy and hepatic steatosis, adipose tissue accumulation, retinopathy,

exercise intolerance and neuropathy (Wilcken, 2010) (Waisbren, Landau, Wilson, & Vockley, 2013).

## 1.2 Apoptosis

Apoptosis is a programmed cell death process that maintains cell homeostasis during growth and development by eliminating severely damaged cells. In early phase of apoptosis, mitochondria activate the release of caspases by initiating caspase cascade resulting in pro-apoptotic signaling as a death response (Solary, Bertrand, Kohn, & Pommier, 1993) (Gavrieli, Sherman, & Ben-Sasson, 1992). Caspases are found as inactive proenzymes, during apoptosis, the activation of the caspase is required to cleave many proteins out of the mitochondrial membrane. After caspase activation, morphological changes occur like cell shrinkage, nuclei condensation, and DNA fragmentation. Then, vital caspase substrates in the cells is cleaved by the active caspase's resulting in the release of apoptotic bodies, which spread rapidly as a result of phagocytosis of neighboring cells. Apoptosis occurs primarily via two main pathways namely extrinsic and intrinsic pathway of apoptosis as illustrated in **Figure 1**. Both pathways are initiated by different mechanisms and signals which activate the caspases 3 and 7 that cleave more than 1000 proteins leading to changes in cell morphology indicating apoptosis (Kalkavan & Douglas, 2017).



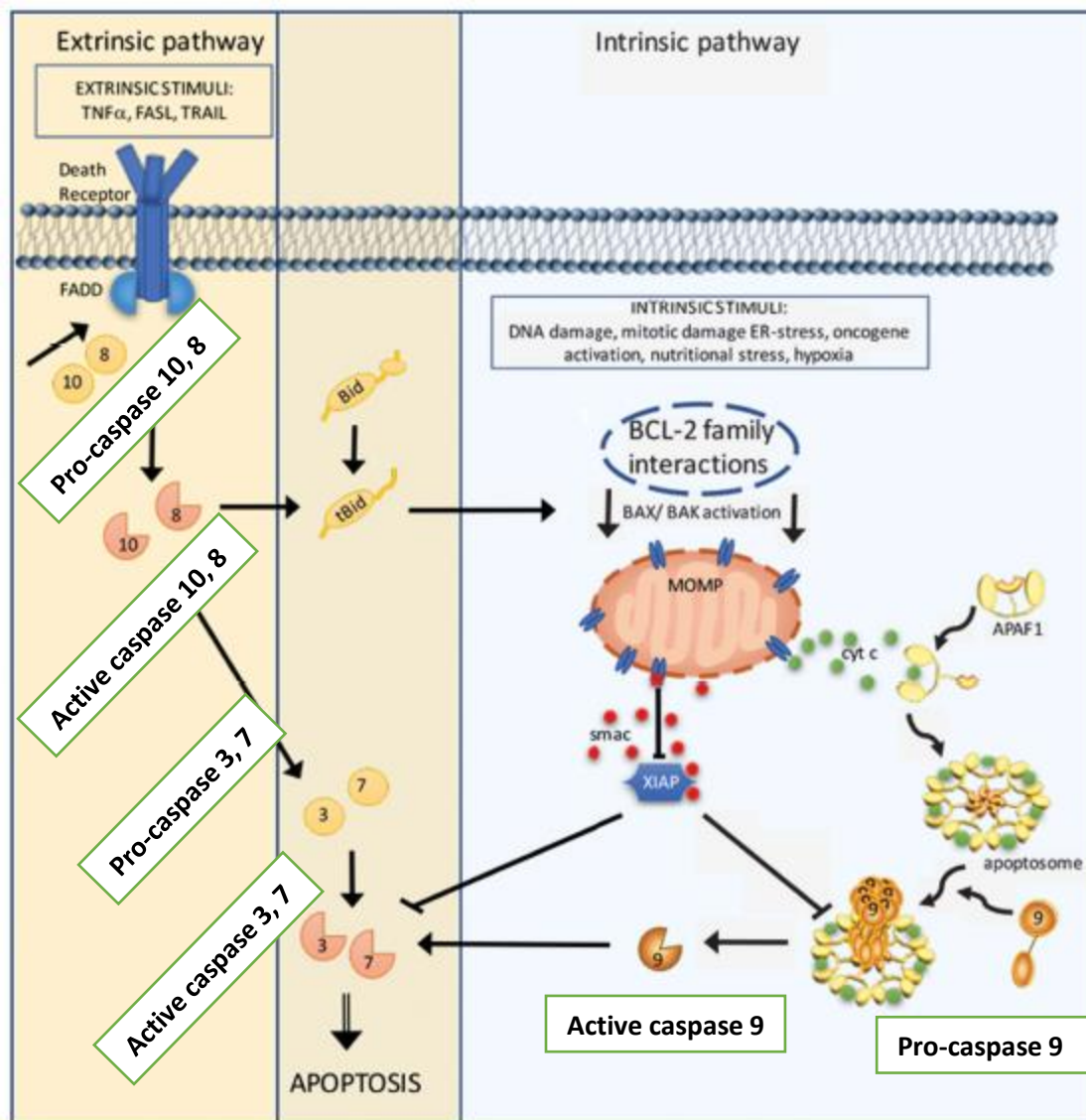


**Figure 1 The extrinsic and intrinsic apoptotic pathways.** At the plasma membrane, extrinsic pathway is activated when death receptors ligands bind to a subset of tumor necrosis factor receptor (TNF) receptors including TNFR1, Fas receptor, and death receptors. These receptors activate the procaspases 8 and 10 which leads to the activation of caspase 3 and 7 resulting in apoptosis. Intrinsic pathway is modulated by cell stressors such as Endoplasmic reticulum stress, DNA damage, nutritional stress and hypoxia. Mitochondrial outer membrane permeabilization (MOMP) occurs via the interaction of pro-apoptotic BH3 containing proteins such as BAX and BAK and BAX/BAK oligomerization. Pro-apoptotic intermembrane space (IMS) releases Cytochrome c (Cyt c) and second mitochondria-derived activator of caspase (SMAC) resulting in activating procaspase 9. Active caspase 9 cleaves pro-caspase 3 and 7 resulting in their activation for caspase-dependent apoptosis. This figure is adopted and modified from (Kalkavan & Douglas, 2017).

### ***1.2.1 Extrinsic and Intrinsic Pathway of Apoptosis***

The extrinsic pathway or death receptors pathway of apoptosis is initiated by the activation of death receptors (DRs) at cell membrane including tumor-necrosis factors (TNF), TNFR1, Fas receptor, CD95, and TRAIL receptors, respectively. These receptors play a critical role in communicating death signals from cell surface into mitochondria (Saraste, 1999). Once the subset of these receptors is activated by ligand binding in the plasma membrane, the activation of procaspase-8 or 10 takes place leading to their substrate caspase 3 and 7 cleavage and activation for the induction of apoptosis.

The intrinsic pathway of apoptosis is a response to internal damage and stressors such as damaged DNA, damaged chromosome, and ER- stress. As a result of the cell sensation to the internal stressors, the interaction of BCL-2 family members such as the activation of BH3 domain containing pro-apoptotic proteins; BAX and BAK, and results in the formation of mitochondrial outer membrane permeabilization pore (MOMP). Consequently, the releases of apoptogenic factors such as cytochrome c, second mitochondria-derived activator of caspases (SMAC) (Kroemer et al., 2009) and apoptosis-inducing factor (AIF) from the mitochondria are induced (Kalkavan & Douglas, 2017; Saraste, 1999) . These proteins induce caspase dependent and independent cell death by generating reactive oxygen species (ROS) and cytochrome which eventually trigger caspase 3 activation. The activated caspases cleave proteins that stimuli apoptosis and result in abnormalities in genome DNA. However, both

intrinsic and extrinsic pathways activate caspase cascade leading to programmed cell death.

### **1.3 Mitochondria**

Mitochondria is an important organelle to maintain cellular homeostasis, to produce adenosine triphosphate (ATP), to regulate redox and calcium homeostasis, cellular metabolism, and apoptosis. Mitochondria has unique function for lipid metabolism where fatty acids oxidation takes place. The integrity and the quality of mitochondria are controlled through many cellular and molecular pathways (Radek et al., 2014). Mitochondria is considered as a clock that affect the lifespan of cellular processes, any disturbance in the mitochondrial function can result in the development of metabolic disorders (Blagosklonny, 2008). Defect in mitochondrial performance results in altered redox hemostasis leading to the generation of reactive oxygen species (ROS) (Radek, Marco, & Heinz, 2014). Further, mitochondria have also been demonstrated to regulate intracellular signaling via  $Ca^{2+}$  and ROS (Tait & Green, 2012). Abnormal levels of ROS generation can impact the mitochondrial processes causing a disruption in respiratory chain, and activate apoptotic process (Friedman & Jodi, 2014). It is important to control mitochondrial integrity to maintain cellular homeostasis. The manifestation of a variety of human diseases can impair the quality control system of the mitochondria.

### **1.3.1 Mechanisms of Mitochondria in Inducing Pathophysiology**

In LCHAD disorder, the mitochondria are involved in mechanisms of inducing apoptosis and lipotoxicity. Although energy deficiency seems to play a major role in development of pathophysiology especially in hepatopathy cardiomyopathy of the affected patients (Wilcken et al., 2007) and skeletal myopathy (Spiekerkoetter et al., 2010), central and peripheral neuropathy are not associated with caloric intake and hypoglycemia (Wajner & Umpierrez, 2016). Therefore, it is possible that there are mechanisms other than energy deficiency could contribute to the pathogenesis of LCHAD deficiency. It has been suggested that mitochondrial stress and accumulation of metabolites compounds such as fatty acids and carnitine might be the mechanisms that induce pathogenesis in LCHAD deficient individuals (Spiekerkoetter & Wood, 2010); (Olpin, 2013).

Wajner *et al.*, summarized the recent evidences of the mechanisms that affect energy homeostasis and lead to pathophysiology. The gathered data was based on patients and animal models with mitochondrial disorders suggesting that the mechanisms to disorders might be redox reactions, fatty acid accumulation, calcium homeostasis, and energy deficiency. **Figure 2** illustrates the major roles of accumulated fatty acids metabolites inducing lipotoxicity resulting in energy and mitochondrial damage (Wajner & Umpierrez, 2016). LCHAD deficient individuals develop mitochondrial dysfunction and energy deficiency. Further, biochemical and mitochondrial morphological alterations were also observed in LCHAD deficient patients' heart, skin fibroblasts, and

muscle tissues (Derks et al., 2014);( Najdekr et al., 2015);( Feillet et al., 2003);(Wakabayashi et al., 2012); (Ruitenbeek et al., 1995).

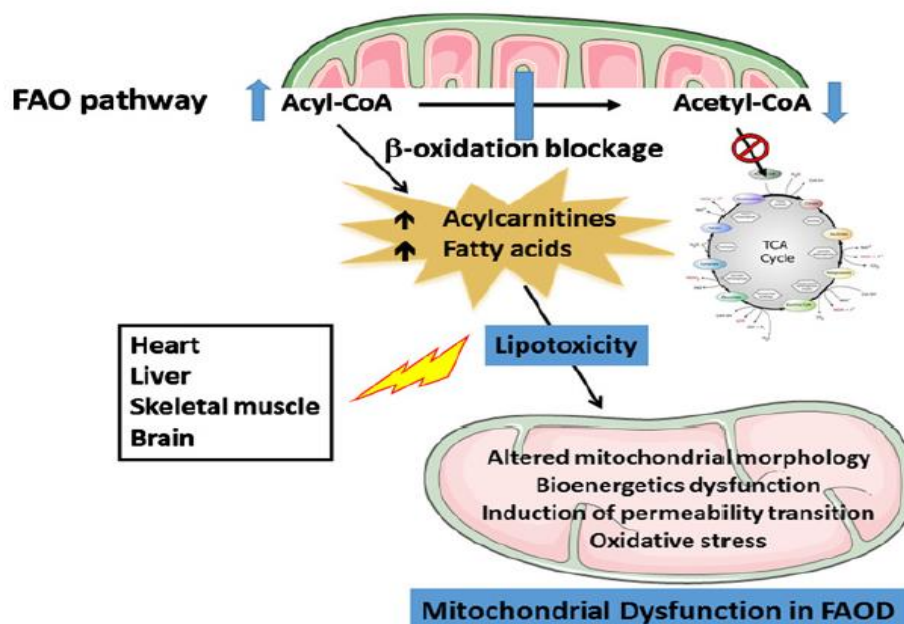


**Figure 2 Mitochondrial dysfunction provoked by fatty acids and acyl carnitines accumulating in FAOD.** In defective fatty acid oxidation (FAO) pathway, the acyl-CoA can't be converted into Acetyl-CoA resulting in higher accumulation of the substrates such as acyl carnitines and fatty acids. The accumulation of these compounds is toxic to the heart, liver, muscle, and brain tissue's that rely on fatty acids for energy. This lipotoxicity alters the mitochondrial bioenergetic functions and increases oxidative stress. This figure is adopted from (Wajner & Umpierrez, 2016).

Further, oxidative phosphorylation (OXPHOS) takes a place in the mitochondria to produce ATP and reactive oxygen species (ROS) through respiration chain. The ROS plays an important role in regulating gene and enzyme activity, increased free radical production and decreased ATP-production would lead the cells to a cascade of apoptosis or necrosis (Natarajan, Eapen, Pullimood, & Balasubramanian, 2006). Collectively, these published evidences ensure how mitochondria and energy disturbance are associated with

pathophysiology in the tissues that primarily rely on the mitochondrial fatty acid  $\beta$ -oxidation like LCHAD deficient patients.

### **1.3.2 Role of Mitochondria in Fatty Acid Oxidation Disorder**

Individuals with LCHAD deficiency accumulate lipotoxic compounds such as fatty acids and acyl carnitines in the systemic circulation and tissues which might induce cellular lipotoxicity (Lipoapoptosis). There are many evidences supporting the role of accumulated fatty acids and acyl carnitines compounds in distressing mitochondrial homeostasis mainly on the brain, liver, and skeletal muscle. Meyer et al., isolated retinal cells from early forebrain populations and they used hiPSC cultures showing that excessive lipid load in non-adipose cells such as retinal pigmented epithelial (ARPE) cells can impair normal cell signaling leading to peroxidation, cellular dysfunction, and apoptotic cell death (Meyer et al., 2011). Although non-adipose cells such as ARPE cells have limited capacity for lipid storage, LCHAD deficient retinal cells have shown lipid accumulation resulting in retinal atrophy (Meyer et al., 2011). Further, medium-chain acyl-CoA deficiency (MCAD) results in the accumulation of medium fatty acids like octanoic acid, decanoic acid, and cis-4-decanoic acid. These accumulated medium chain fatty acids results in mitochondrial damage and induces BAX-BAK oligomerization resulting in pore formation in the mitochondrial outer membrane and alters the mitochondrial permeability transition (mPT) (Parker, W., Haas, Stumpf, & Eguren, 1983); (Schuck, Ferreira Gda et al., 2009); (Schuck et al., 2010); (Schuck, Ferreira et al., 2009). Wajner *et al*, postulated that LCHAD

deficient accumulate 3-hydroxy fatty acids like 3-hydroxydodecanoic acid, 3-hydroxy myristic acid, and 3-hydroxy palmitic acid. Further, in LCHAD deficient animals, it was shown that hydroxy fatty acids can disturb energy and redox homeostasis (Wajner & Umpierrez, 2016). These hydroxy fatty acids were shown to uncouple mitochondrial oxidative phosphorylation (OXPHOS), induces mPT and oxidative stress leading to the pathophysiology of cardiac, hepatic, and myopathic in LCHAD deficient individuals. In addition to hydroxy fatty acids, carnitine derivatives also accumulate in tissue causing disturbance to the mitochondria and  $\text{Ca}^{+2}$  homeostasis (Wajner & Umpierrez, 2016). Further, lipotoxic lipid metabolites induces mitochondrial abnormalities leading to many events including uncoupling of OXPHOS, decreases respiratory chain activity, and nicotinamide adenine dinucleotide (NAD<sup>+</sup>) levels (Touma & Charpentier, 1992); (Trauner, Nyhan, & Sweetman, 1975).

Our lab has previously published that long-chain fatty acids *e.g.*, palmitic acid and arachidonic acid were elevated during acute fatty liver of pregnancy (AFLP) or LCHAD deficiency. We also have unpublished data on the mechanism of 3-hydroxy fatty acid-induced hepatocyte lipoapoptosis (Natarajan & Ibdah, 2018). Further, our lab has also established the lipotoxic role of palmitic acid in causing hepatocyte and cholangiocyte lipoapoptosis by the activation of mitogen-activated protein kinase (MAPK), and forkhead family of transcription factor class O3 (FoxO3) dependent pro-apoptotic signaling pathway (Natarajan et al., 2014); (Natarajan et al., 2017). Another study demonstrated that the major accumulating lipotoxic metabolites during LCHAD deficiency is 3-hydroxymyristic acid (3-HMA)

and 3-hydroxypalmitic acid (3HPA) in the circulation and these 3-hydroxy fatty acids were also found to accumulate in different tissues, and significantly affect mitochondrial homeostasis (Hickmann et al., 2015). Collectively, it has been demonstrated that the lipotoxicity of 3-hydroxy fatty acids and acyl carnitine metabolites were more likely to be involved in the pathogenesis of LCHAD deficient individuals.

#### **1.4 Retinal Pigmented Epithelial Cells in LCHAD Deficiency**

Retinal pigmented epithelium (ARPE) is a monolayer of cells that are the main nutrient provider for the retina in eye. Melanin display potential antioxidant roles including inhibition of oxidation, remove redox-active metal ions, and protect against free radicals in retinal pigment epithelium (RPE). Development of retinopathy is highly associated with LCHAD deficiency but not with other fatty acid oxidation disorders (FAODs) (Padmini et al., 2015). The LCHAD inherited deficiency has been reported to develop pigmentary retinopathy leading to vision loss without early intervention, high myopia, poor vision, and chorioretinal atrophy (Tyni et al., 1998). Tyni *et al.*, have also demonstrated the fatty acid oxidation enzymes in retinal pigment epithelial cells including carnitine palmitoyl transferase (CPT-I and CPT-II) and all mitochondrial beta-oxidation enzymes (Tyni, Paetau, Strauss, Middleton, & Kivela, 2004).

The pigmentation in RPE tends to decrease with aging leading to vision degradation (Padmini et al., 2015) and patients with LCHAD deficiency develop different stages of pigment retinopathy (Tyni, Immonen, Lindahl, Majander, &



Kivela, 2012). Further, severity of retinopathy and staging for chorioretinopathy were documented in LCHAD deficient individuals. The RPE of patient with LCHAD deficiency at early stage showed retinopathy with less pigmentation and less atrophy. The RPE of patient with LCHAD in advance stage displayed severe retinopathy, dramatic pigmentation and damage in the retinal cells. However, the mechanism behind the retinopathy in LCHAD deficiency is still unclear. Also, it has been suggested that the accumulation of toxic long chain fatty acids (LCFA) and 3-hydroxy fatty acids (3-HFA) might be a possible mechanism behind retinopathy (Den et al., 2002);(Schrijver-Wieling et al., 1997). Based on this literature we hypothesized that defective mitochondrial fatty acid  $\beta$ -oxidation and the accumulation of 3-hydroxy fatty acid in the retinal epithelium can induce the development retinopathy in LCHAD deficient individuals.

#### **1.4.1 Apoptosis of Retinal Cells in LCHAD Deficiency**

Padmini et al., has isolated human induced pluripotent stem cell (hiPSC) from LCHAD deficient individuals and differentiated hiPSC into RPE cells to create LCHAD deficient *in vitro* culture model (Padmini et al., 2015). These cells were derived from patients with homozygotes mutation in *HADHA* gene. The study compared control RPE cells to the cells derived from LCHAD deficient individuals and characterized the RPE cell structure and functional alterations. The differentiated RPE from LCHAD deficient individuals displayed increased lipid accumulation, less pigmentation, few melanosomes, retinal atrophy and increased RPE apoptosis. They also observed mitochondrial damage and

decreased mitochondrial oxidant scavenging are potential as a mechanism of retinopathy. In summary, PRE cells from patients with LCHAD deficiency showed mitochondrial damage increased lipid accumulation, decreased melanosome, and apoptosis.

## **1.5 Dietary Supplementation as a Protective Strategy Against LCHAD Deficiency**

The main strategy for patients with LCHAD deficiency is to avoid energy complications. Dietary management of LCHAD involves long chain fatty acids (LCFA) restrictions and avoids catabolic crises such as fasting by giving adequate supply of calories from carbohydrate and medium chain fatty acids (MCFA) (Wajner & Umpierrez, 2016). However, giving glucose polymers is not recommended to be supplemented habitually, instead, oral prophylactic is suggested for emergency treatment (Spiekerkoetter et al., 2009). To prevent or slow the progression of chorioretinopathy and other pathologies that are associated with LCHAD deficiency, patients are recommended to follow a very low-fat diet (10% of total energy) supplemented with medium chain fatty acids (MCFA) (10% of energy) (Wajner & Umpierrez, 2016).

### ***1.5.1 Medium Chain Fatty Acid (MCFA) Supplementation***

Exercise requires higher energy supply, it has been reported that MCFA supplementation is enough to provide sufficient energy for prolonged period of exercise in patients with very long-chain acyl-CoA deficiency (VLCAD) (Spiekerkoetter, 2007). Therefore, supplementing with MCFA is important for

optimal health needs for VLCAD deficient individuals (Lindner et al., 2009). Further, the destruction of muscle cells that are resulted from exercise can be inhibited by taking adequate amount of MCFA before the exercise in LCHAD deficient individuals (Gillingham, Scott, Elliott, & Harding, 2006). Since the fat intake is restricted, patients with LCHAD need to be supplemented with fat-soluble vitamins. In addition, Triheptanoin (UX007) is a drug composed of medium chain triglyceride that possesses the gluconeogenic and ketogenic role because it provides alternative substrates during increased energy needs and during fasting. It has been shown that UX007 can reduce hypoglycemia, rhabdomyolysis, and cardiac functions and improves endurance exercise and tolerance in patients with severe LCHAD deficiency (Vockley et al., 2017).

### ***1.5.2 Carnitine Supplementation***

Carnitine supplementation might be beneficial for detoxification of the toxic 3-hydroxy fatty acids and long chain fatty acids compounds from the circulation (Spiekerkoetter & Wood, 2010). On other hand, L-carnitine was found to worsen the health by accumulating toxic long-chain carnitine substrates (Treem et al., 1996); (Rocchiccioli et al., 1990). However, further study needs to be explored to understand the protective role of carnitine against lipotoxic 3-hydroxy fatty acids metabolites in retinal pigment epithelial cells.

### ***1.5.3 Docosahexaenoic Acid Supplementation***

The beneficial role of docosahexaenoic acid (DHA) has been explored in a prospective cohort study for the retinal function in children's with LCHAD deficiency. The authors demonstrated that DHA-supplemented patients with LCHAD deficiency showed reduced the retinal complications (Gillingham, Weleber, & Neuringer, 2005). It was also demonstrated that the severe progression of chorioretinopathy was associated in patients with elevated 3-hydroxy-acylcarnitines. Further, levels of 3-hydroxyacylcarnitines and 3-hydroxy fatty acids were directly proportional with severity of retinal atrophy (Gillingham et al., 2005); (Jones et al., 2000); (Jones et al., 2001). These data suggest the 3-hydroxy fatty acids is toxic to the retina and RPE cells and supports our hypothesis of the present study.

The dietary recommendations for LCHAD deficient patients highlighted in the previous sections are still not a mechanism based. Additionally, many patients still experiencing hospitalization due to shortage in energy supply and accumulation of toxic 3-hydroxy fatty acids compounds (Kinman et al., 2006; Roe & Brunengraber, 2015). Our long-term goal is to develop a nutraceutical approach to prevent 3-hydroxy fatty acid-induced retinal pigment epithelium damage.

### ***1.5.4 Protective Role of Palmitoleate Supplementation***

Palmitoleic acid (PO) is a monounsaturated omega-7 fatty acid that present in animal fat, plant oil, and macadamia nuts. It can be synthesized from

palmitate C16 (saturated fatty acid) by the enzyme stearoyl CoA-desaturase (SCD1). PO is involved in many processes associated with cell function such as growth, signaling, storage, and cell differentiation. It has been demonstrated that PO acts as anti-apoptotic fatty acid that improves lipid profile in metabolic disease animal models (Morgan, Dhayal, Diakogiannaki, & Welters, 2008); (Morgan & Dhayal, 2010). Zhi-Hong Yang *et al.* showed antidiabetic effect of PO in *KK-Ay* mice that developed diabetes and hyperglycemia. Further, PO enriched diet has been demonstrated to protect pancreatic beta cells from apoptosis, improved hypertriglyceridemia, glycemic control, glucose uptake, and prevented lipid accumulation in the liver in *KK-Ay* mice (Yang, Z. H., Miyahara, & Hatanaka, 2011). In comparison to palmitic acid (PA) a saturated fatty acids, PO has more protective role against hepatic lipotoxicity and placental lipotoxicity (Yang, H., Miyahara, & Hatanaka, 2011); (Yang, Z. H. et al., 2011). Additionally, Yang *et al.*, investigated in animals by orally administered vehicle (control), 300 mg/kg per day of PA, or 300 mg/kg per day PO for 4 weeks to show the effect of palmitoleic acid on hepatic steatosis in *KKAy* mice. PO dramatically reduced lipid accumulation in the liver of diabetic mice compared to control and PA supplementation. In addition, PO supplementation also controlled lipogenesis and prevented lipid accumulation in adipose tissue

## **1.6 Central Hypothesis, Purpose, and Specific Aims**

### ***1.6.1 Central Hypothesis and Purpose***

Retinopathy is very common characteristic in patients with LCHAD deficiency that is not observed in other fatty acid oxidation defects. The retinal damage in LCHAD deficient patients is associated with retinal pigmentation, peripheral neuropathy, and cognitive deficiency (Tyni, Paetau, Strauss, Middleton, & Kivela, 2004) (Natarajan & Ibdah, 2018). However, the molecular mechanism behind the retinopathy in LCHAD deficiency still unclear.

Identification of the lipotoxic role of 3-hydroxy fatty acids (3-HFAs) may offer new perspectives for potential mechanism and to develop new therapeutic dietary strategies to LCHAD deficient patients. Hence, we hypothesize that the increased levels of toxic 3-hydroxy fatty acid metabolites in LCHAD deficiency can induce lipoapoptosis in retinal pigment epithelial cells. Despite the dietary recommendations for patients with LCHAD with medium chain fatty acids (MCFAs) supplementation, patients still experiencing hospitalization due to shortage in energy supply and accumulation of toxic 3-HFAs metabolites. Because MCFAs can be elongated to form long chain fatty acids (LCFAs). Therefore, future prospective studies and development of approved treatment strategies are needed. In terms of nutritional or dietary therapy, it has been shown that palmitoleic acid (PO) has a beneficial role against lipid accumulation in liver of diabetic mice and it also plays a protective role against hepatic lipid droplets accumulations. We further hypothesized that PO protects against 3-HFAs induced retinal pigmented epithelial (RPE) cells lipoapoptosis.

This master thesis underlines how the accumulated 3-hydroxy fatty acids (3-HFAs) contribute to retinal pigment epithelial cell damage. To further understand the mechanism of the damage, this study aimed to identify the molecular mechanism of the 3-HFA-induced retinal pigment epithelial cell lipotoxicity using human immortalized adults retinal pigmented epithelial cells (ARPE-19). Further, the protective role of palmitoleic acid (PO) in reducing lipid accumulation in retinal cells is also investigated. Further the role of p53 upregulated modulator of cJun N-terminal kinase (JNK) in 3-HFAs-induced RPE lipoapoptosis is also investigated.

### **1.6.2 Specific Aims**

The specific research objectives of this thesis are as follows:

- **Specific Aim 1:** We will determine the mitochondrial bioenergetics of retinal pigmented epithelial cells (ARPE-19) cells with 3-HFAs exposure.
- **Specific Aim 2:** We will detect the role of 3-HFAs in inducing cell apoptosis in ARPE-19.
- **Specific Aim 3:** We will detect the lipid droplet accumulation in ARPE-19 cells with 3-HFAs treatment.
- **Specific Aim 4:** We will elucidate the mechanism of 3-HFA-induced ARPE cell lipoapoptosis is via caspase and JNK activation.

## 2. CHAPTER II: MATERIALS AND METHODS

### 2.1 Cell Culture

#### 2.1.1 Sub-Culturing Cells

Cell cultures were performed using normal human retinal pigmented epithelial cells (ARPE-19) that were purchased from ATCC. The ARPE-19 were grown as monolayer in medium Dulbecco's Modified Eagle's Medium (DMEM) containing serum-supplement with 10% of FBS (fetal bovine serum), HEPES (4-(2-hydroxyethyl)-1-piperazineethanesulfonic acid) (15 mM) , sodium pyruvate (0.5 mM) , and sodium bicarbonate (1200 mg/L). The cells were seeded in flask with growth media and cultured in an environment with 5% CO<sub>2</sub> at 37 °C. For sub-culturing the cells; media was discarded using aspirator, the cells were rinsed with PBS and incubated 1 mL of Trypsin for 1-2 minutes to allow the cells to detach from the flask. After that, 5 mL of growth media was added, and cells were re-suspended and cell suspension were centrifuged 500 x g for 5 minutes to remove the supernatant and the cell pellets were resuspended with fresh media and plated in new culture flask.

#### 2.1.2 Counting Cells

The cells were counted using hemocytometer was placed under the microscope with 10X objective to visualize the cells located in the chambers indicated by gridlines square. **Figure 3 (A)** shows a schematic of the location of the counted cells inside the chamber. After counting the cells in both chambers,



the cells were averaged then multiplied by the following factors: dilution factor (10X), mL-conversion factor (1000), and number of squares that contained counted cells as shown in **Figure 3 (B)**.

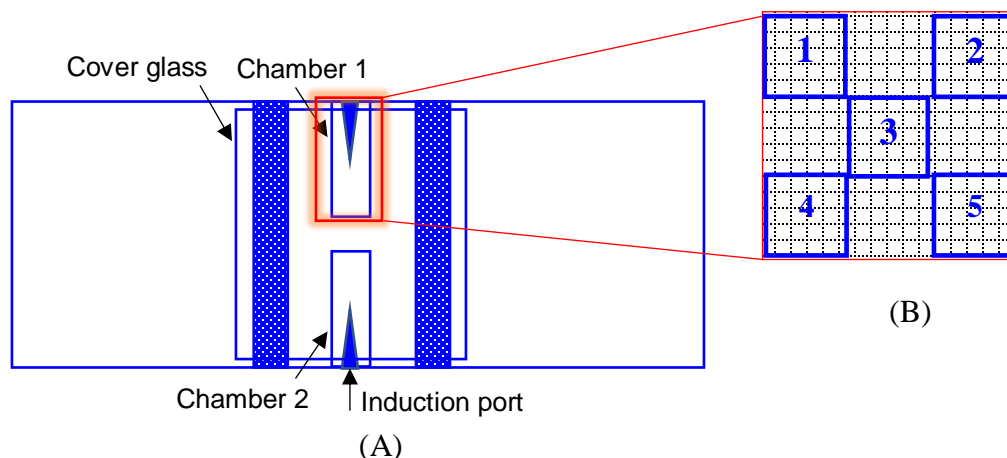


**Figure 3** Schematic of (A) Hematocytometer and (B) counting chamber.

### 2.1.3 Cell Seeding

ARPE-19 cells were seeded at density of 60,000 cells/well in 24-well plate and 10,000 cells/well in 96-well plate containing DMEM media with volume of 500  $\mu$ L/well in 24-well plate and 100  $\mu$ L/well in 96-well plate, respectively. Treatment of different 3-hydroxy fatty acids or fatty acids were performed after the cells were attached to the plate.

### 2.2 Fatty Acids Preparations

Different types of fatty acids were used in the present study: 3-hydroxy fatty acids (3-hydroxy palmitic acid and 3-hydroxy myristic acid), saturated fatty acids (palmitic acid and myristic acid), and palmitoleic acid were treated as described below.

### 2.2.1 Treatment of 3-Hydroxy Fatty Acids (3-HFA)

The experiment was designed with two different conditions including a vehicle control and 3-HFAs treatment. The vehicle cells were treated with only isopropanol and 1% of bovine serum albumin (BSA) obtained from Millipore Sigma. The ARPE-19 cells were treated with two different types of 3-HFA: 3-hydroxy palmitic acid (3-HPA) and 3-hydroxy myristic acid (3-HMA), both were purchased from Cayman Chemical Company. These 3-hydroxy fatty acids were dissolved in isopropanol with a stock solution of 80  $\mu\text{M}$ . To treat the cells with 3-HFA, 1% BSA containing growth media were preincubated at 37°C for 30 minutes and filter sterilized. BSA-containing media was is mixed with 3-HFA and incubated at 37°C for another 20 minutes prior to the treatment.

The experiment was designed to treat ARPE-19 cells with different concentrations of 3-HFA (150, 200, and 250  $\mu\text{M}$ ) for 24 hours as shown in **Figure 4**. After seeding the cells, the growth media was removed using aspirator then 3-HFA containing media were added to the wells.

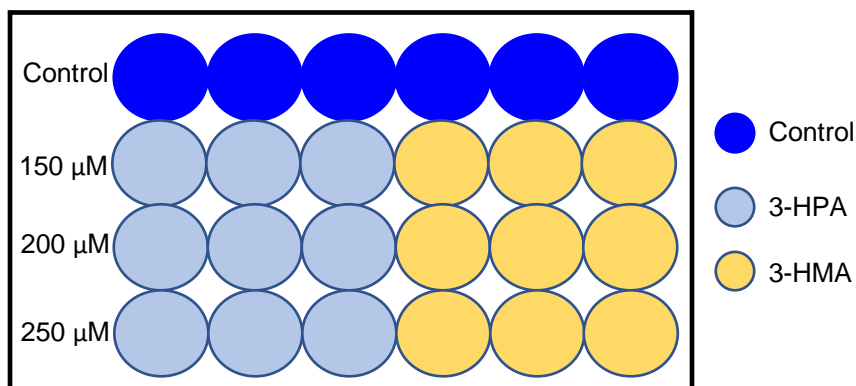


**Figure 4** 24-well format of a control and 3-HFA treatment in ARPE-19 cells.

### **2.3 Apoptotic Nuclear Morphological Changes**

Biochemical apoptotic nuclear morphological changes were detected after 24 hours of 3-HFAs treatment. Apoptotic morphology changes can be visualized under microscope and that duration of time is varying based on cell type (Saraste, 1999). Control and treated cells were stained with 5 µg /ml DNA-binding dye, DAPI (4',6-diamidino-2 phenylindole) for 20-30 minutes at 37 °C. Nuclear images were obtained using epifluorescence microscopy using an EVOS FL inverted microscope. Apoptotic nuclei were counted and presented as a percent of total nuclei. At least 100 cells were counted per well and experiments were performed in triplicate.

### **2.4 Measurement of Caspase 3/7 activity**

Caspase 3/7 activity was measured by enzymatic fluorophore release (Apo one, Promega, TB323) according to the manufacturer's instruction (Promega) and represented as fold change compared to vehicle treatment, with experiments performed in quadruplicate as described (Promega, TB323). Briefly caspase substrate and buffer were mixed with 1:100. After 24 hours of 3-HFA treatment in ARPE-19 cells, mixed reagents (caspase substrate and buffer) were added. To detect the enzymatic fluorophore release using Synergy-H1 Hybrid Reader (BioTek)

## **2.5 Mitochondrial Stress**

All materials used in this experiment were provided from Agilent Seahorse using XF Cell Mito Stress test kit. This experiment was carried out at Biomedical and Obesity Research Core (BORC) facility at University of Nebraska-Lincoln. Mitochondrial stress experiment was conducted according to Seahorse protocol (Meerlo, Kaspers, & Cloos, 2011). The procedure includes cells plating, media preparation, stock solutions preparation, and oxygen consumption rate measurement.

### ***2.5.1 Plating Cultures and Hydrating Sensor Cartridge***

ARPE-19 cells were plated in Seahorse XF24 cell culture microplate with 100  $\mu$ l/well density mixed with 150  $\mu$ l/well of DMEM growth media, then cells were incubated in 5% CO<sub>2</sub> incubator for 8 hours for adherence. The sensor cartridge of XF calibration plate was hydrated in 1ml/well of XF calibrant buffer, that was premixed and provided from Agilent Seahorse, then the plate was stored in non-CO<sub>2</sub> incubator overnight for sensor calibration.

### ***2.5.2 Preparing Assay Medium***

XF base medium was supplemented with the following nutrients (Sigma); Pyruvate (1 mM), Glutamine (2 mM) and Glucose (10 mM). The base medium was warmed in water bath at 37°C for 5 minutes and the pH was adjusted to 7.4 and followed by filter sterilization. Cells were rinsed twice with the supplemented

base media and stored in non-CO<sub>2</sub> incubator for 1 hour prior to the mitochondrial stress test.

### ***2.5.3 Preparing Stock Compounds***

The Seahorse XF Cell Mito Stress Test Kit includes pouches with three tubes of Oligomycin (1  $\mu$ M), Rotenone (0.5  $\mu$ M), Antimycin (0.5  $\mu$ M), and FCCP (0.5  $\mu$ M). Each compound was pipetted into 15 mL experiment tube with 3 mL of XF base media with the following amounts; Oligomycin (1.24  $\mu$ L), FCCP (0.67  $\mu$ L), and Rotenone/Antimycin (1.5  $\mu$ L). The previous volumes were calculated according to table 5 in Seahorse protocol (Agilent Technologies, 2017). The sensor cartridges were loaded with the prepared compounds into the appropriate ports as described in the manufacture protocol (Agilent Technologies, 2017; Agilent Technologies, 2018).

### ***2.5.4 Running XF Assay and Measurement of Oxygen Consumption Rate (OCR)***

The XF calibration plate was removed from the non-CO<sub>2</sub> incubator and placed in Agilent Seahorse analyzer instrument tray for calibration for 10 minutes. After that, calibration plate was replaced by XF cell culture plate to obtain oxygen consumption rate (OCR) measurement. The data of OCR for the control and treated cells were obtained from Seahorse XF report generator. The obtained data were analyzed following Seahorse protocol user guide (Agilent Technologies, 2017).

## **2.6 Western Blotting**

### **2.6.1 Protein Isolation**

Control and 3-hydroxy fatty acid-treated cells were washed with 3-5 mL of cold phosphate buffered saline (PBS). Then, 1 mL of lysis buffer containing HEPES, NaCl, tris—HCl and protease inhibitor mixture was added to the washed cells. The cells were scraped with cell scraper, transferred into microcentrifuge tubes and incubated for 40 minutes to complete cell lysis. Cell lysates were centrifuged at 12,000 X at 4°C for 20 minutes. After centrifugation, tubes were placed on ice and the supernatant was transferred into a new microcentrifuge tubes in ice for protein estimation and western blot analysis.

### **2.6.2 Protein Estimation**

Total proteins in cell lysates were quantified using bovine serum albumin (BSA) as standard using pierce 660nm (ThermoFisher) as described in BIO protocol (He, 2011). Briefly, to a 200  $\mu$ L of Pierce protein assay reagent, 2  $\mu$ L of cell lysate and incubated for 5 minutes, then absorbance was measured at OD 595 nm using Synergy-H1 Hybrid Reader.

### **2.6.3 Sodium Dodecyl Sulfate-Polyacrylamide gel electrophoresis (SDS-PAGE) Gel and Immunoblot analysis:**

Protein gel electrophoresis is a technique used to separate the proteins based on their molecular weights through the electrical field to detect the protein of interest. Prior to gel electrophoresis, a 25  $\mu$ L of molecular weight marker and

protein samples were loaded into wells of SDS-PAGE gel (Invitrogen), then placed into electrophoresis apparatus to be electrophoresed for 2 hours at 100 V. Upon applying the electrical voltage, proteins in the wells migrates down through the gel as shown in **Figure 5**.

Next, the gels were transferred to the nitrocellulose membrane (BioRad). The proteins were transferred from the gel to a membrane by making transfer sandwich stack. The sandwich was placed into a transfer tank that filled with transfer buffer (wet method), with 100 V for 1 hour at 4°C. Transferred membrane were blocked with 5% milk powder dissolved in TBST for 1 hour at room temperature prior to immunoblotting detection.

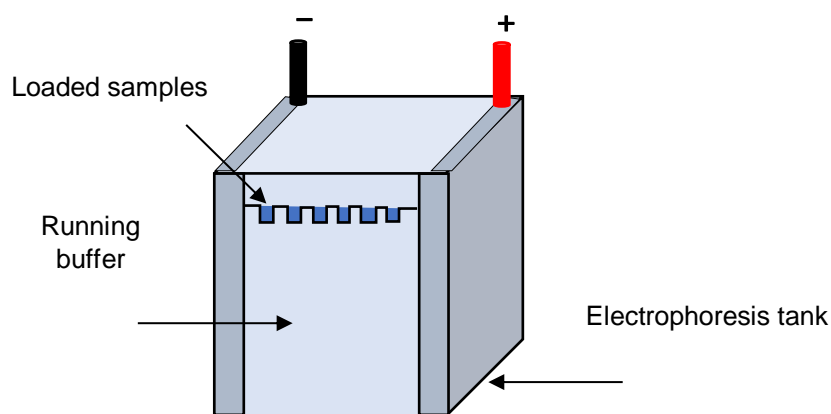


**Figure 5** Schematic representation of SDS-PAGE gel and loading wells.

#### **2.6.4 Immunoblot Detection**

Transferred membranes were incubated at 4°C overnight with primary antibodies against cleaved PARP, Cleaved Caspase 3, and PUMA (1:1000 dilution in 5% milk solution). After that, membrane was washed with TBST three

times with 10 minutes interval. After washing respective secondary antibody conjugated with horse radish peroxidase was added and incubated for 2 hours at room temperature. After washing the membrane with TBST three times for 10 minutes. Detecting membrane bands was accomplished by adding 1 mL of Clarity Western ECL Substrate. Membrane were incubated with 1 ml of solution A & B in Clarity Western ECL Substrate kit containing hydrogen peroxide and luminol were exposed to autoradiography and chemiluminescent images were captured with using ChemiDoc<sup>TM</sup> Touch Imaging System (BIO-RAD).

## **2.7 Oil Red O Staining**

A stock solution of oil red O was prepared by dissolving 0.5 g of oil red O in 100 mL of isopropanol, then the mixture was filtered through whatman filter paper. From the stock solution, 6 mL of oil red O was mixed with 4mL of water. After 24 hours of 3-hydroxy fatty acids treatment, cells were fixed with 2mL/wall of 10% buffered neutral formalin for 30 minutes, then washed with PBS twice. Intracellular lipid droplets in retinal cells were stained with 2mL/ Oil Red O solution at room temperature for 20 minutes, then washed four times with distilled water. Cells were mounted using Fluoromount-G and coverslips and the images were captured using EVOS XL microscope with 40X objective in Dr. Chung' lab in the Department of Nutrition & Health Sciences at the University of Nebraska-Lincoln facility.



## **2.8 Measuring Cell Survival Using 3-(4,5-dimethylthiazol-2-yl)-2,5-diphenyl tetrazolium bromide (MTT) Assay**

To prepare 12 mM stock solution of MTT assay, 1 mL of PBS was added to 5 mg of MTT, then it was vortexed. After ARPE-19 cells were treated with 3-HPA and 3-HMA for 24 hours, the media was removed and 100  $\mu$ L of MTT reagent was added to each well, then incubated for 4 hours. The Formazan formed were with 100  $\mu$ L of isopropanol then stored at room temperature at dark place for 2 hours. The absorbance was measured at OD 570 nm using Synergy-H1 Hybrid Reader (BioTek).

## **2.9 Z-VAD and JNK Inhibitors**

ARPE-19 cells were treated with 3-HPA or 3-HMA or vehicle (Veh) with or without 50  $\mu$ M of pan-caspase inhibitor Z-VAD-fmk (Z-VAD) or JNK inhibitor (SP600125) for 24 hours. Caspase 3/7 activity and cell survival were measured as described above in (E and I).

## **2.10 Statistical Analysis**

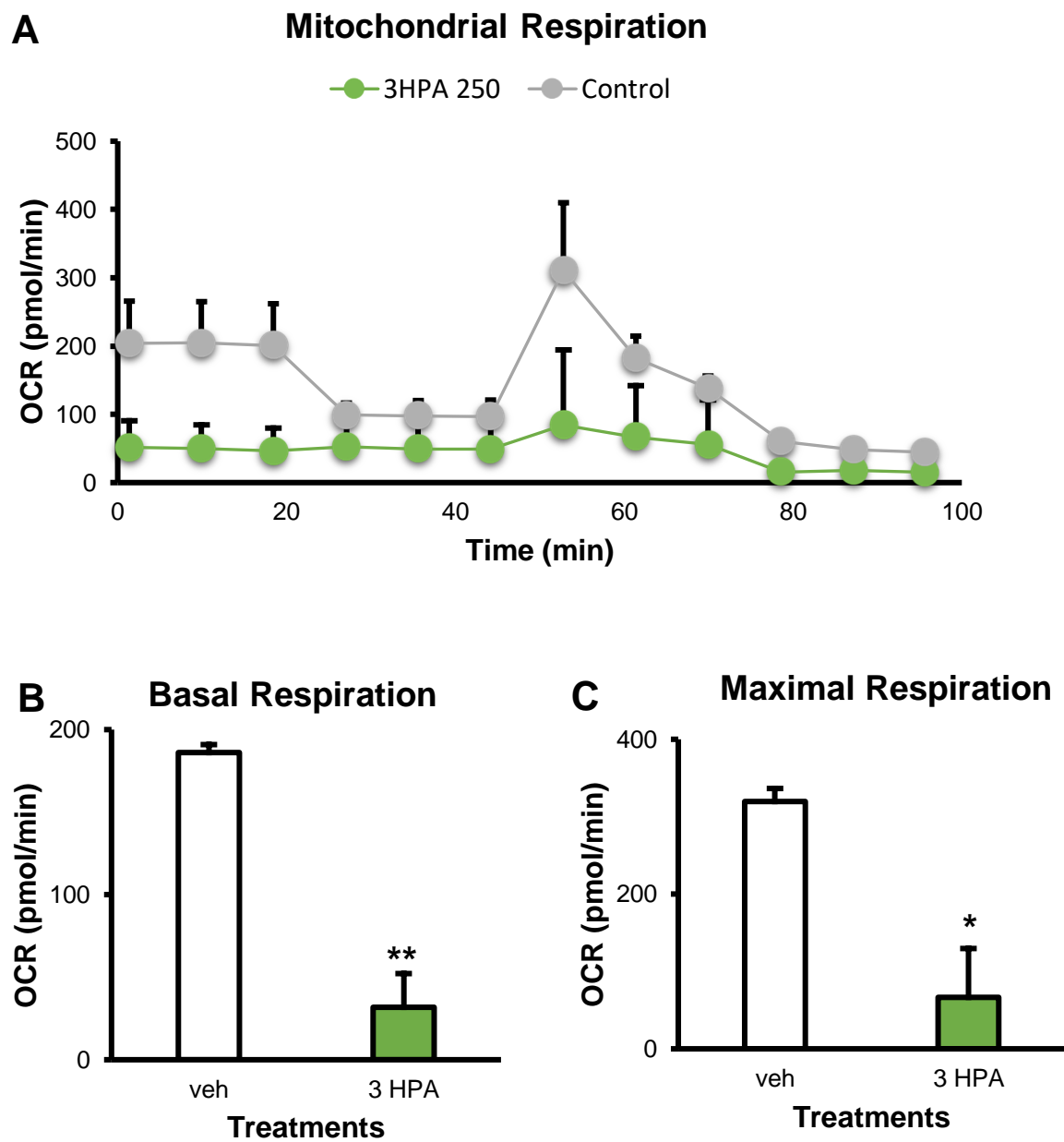
Data were presented as mean  $\pm$  standard error of mean (SEM). The statistical analysis was performed using one-way analysis of variance (ANOVA) with p-value was tested at level 5% \*  $P < 0.05$ . Tukey post hoc correction were carried out to test the statistical significance and to avoid false positives.

### 3. CHAPTER III: RESULTS

#### 3.1 Results

##### **3.1.1 Treatment of 3-Hydroxy Palmitic Acids (3-HPA) Decreased Mitochondrial Bioenergetics in Retinal Pigmented Epithelial Cells (ARPE-19)**

To investigate the effect of 3-hydroxy palmitic acids (3-HPA) on mitochondrial function in retinal pigmented epithelial cells (ARPE-19), *in vitro* mitochondrial stress test was performed to measure oxygen consumption rate (OCR) using Seahorse XF24 Extracellular Flux Analyzer to quantify OCR under basal conditions. Treatment of 3-HPA to ARPE-19 cells resulted in a significant decrease in mitochondrial OCR detected over 100 minutes **Figure 6 (A)**. Further, treatment of 3-HPA to APRE-19 cells showed a significant decrease in basal respiration, maximal respiration, adenosine-triphosphate (ATP) production, and coupling efficiency compared to vehicle (veh) **Figure 6 (B, C, D, and E)**. Vehicle treatment contains equal amounts of isopropanol used to dissolve 3-hydroxy fatty acids in 1% BSA containing media for 24 hours. On the other hand, there was a non-significant decrease in spare respiratory capacity and proton leak in ARPE-19 cells treated with 3-HPA compared to vehicle treatment **Figure 6 (F and G)**. These data suggest that 3-HPA induces mitochondrial damage and results in altered mitochondrial bioenergetics.



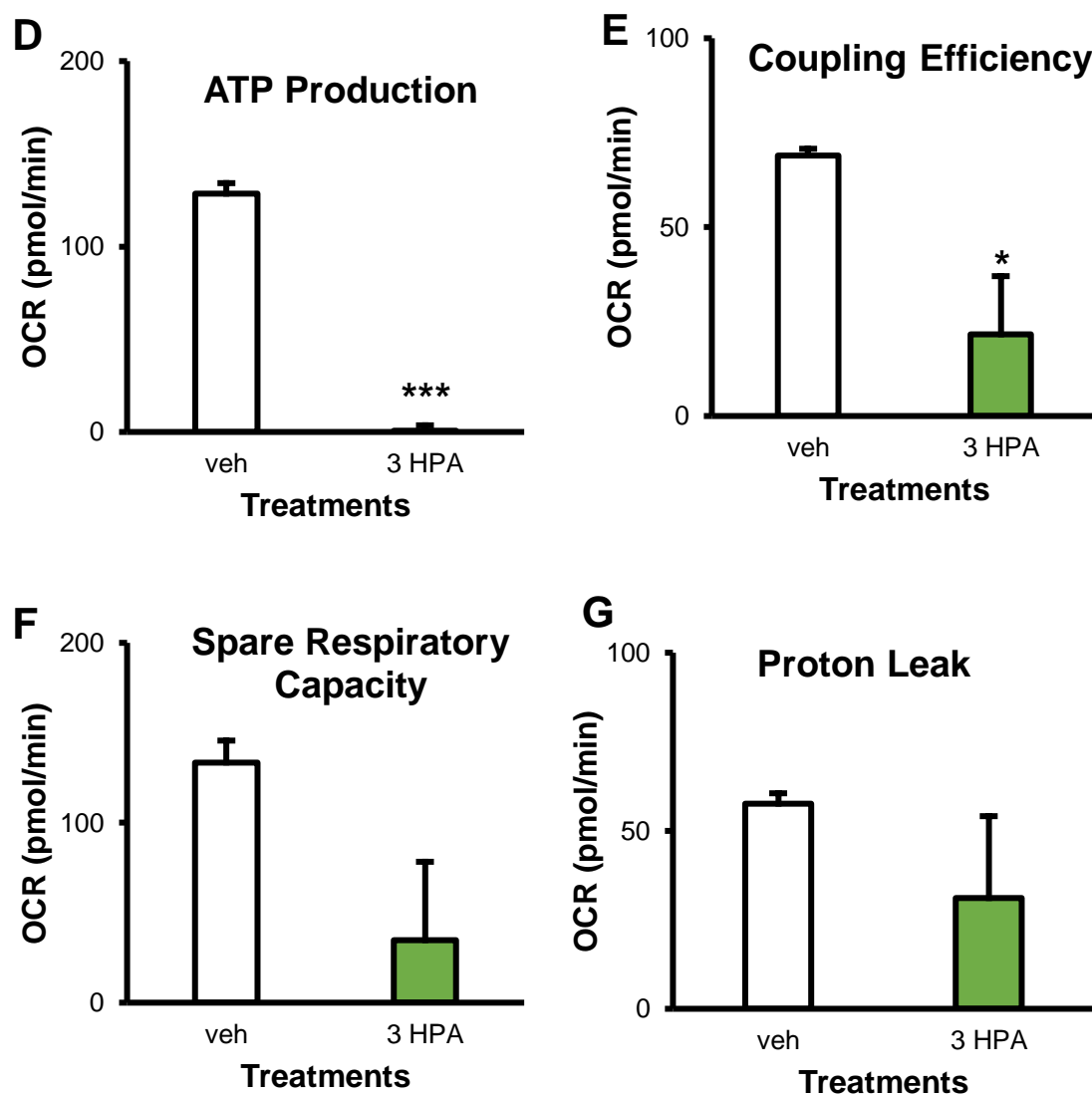


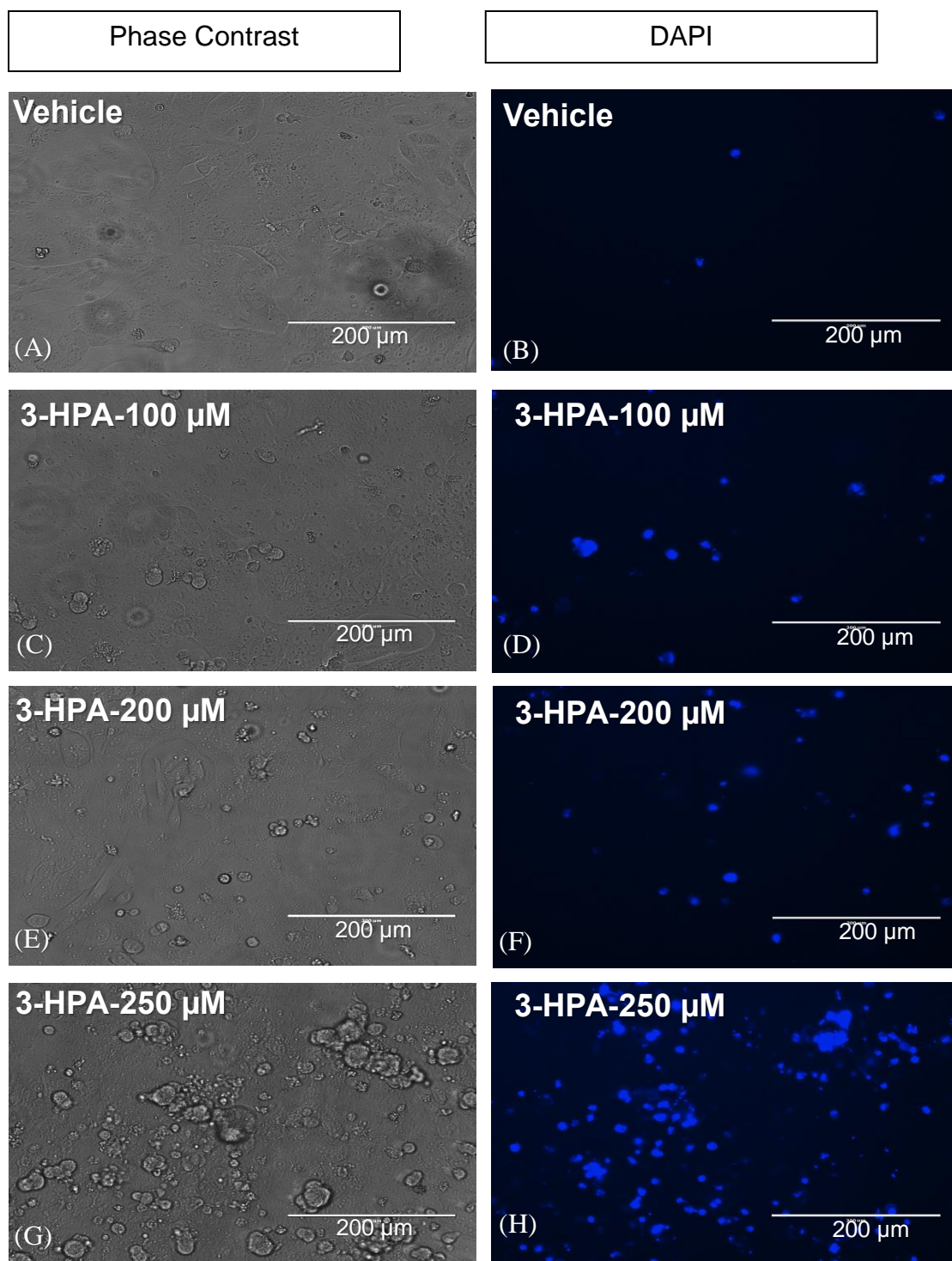
**Figure 6 Mitochondrial bioenergetics functions in ARPE-19 cells treated with 3-HPA.** **A)** Oxygen consumption rate (OCR) for 100 minutes in vehicle and 3-HPA treated ARPE-19 cells. **B)** Basal respiration (**B**), Maximal respiration (**C**), ATP production (**D**), Coupling efficiency (**E**), Spare respiratory capacity (**F**), and Proton Leak of ARPE-19 cells treated with 3-HPA and compared with vehicle ARPE-19 cells, respectively\* indicates P-value with different level of significance compared to vehicle treatment, \*(<0.05). \*\* (<0.01), and \*\*\*(<0.001). The data is represented mean  $\pm$  SEM from five independent experiments, n=5. The statistical significance of the observed differences were obtained by analysis of variance (ANOVA) and Tukey post-hoc test.

### **3.1.2 3-Hydroxy Fatty Acids (3-HFAs) Induce Retinal Pigmented Epithelial Cell (ARPE-19) Lipoapoptosis**

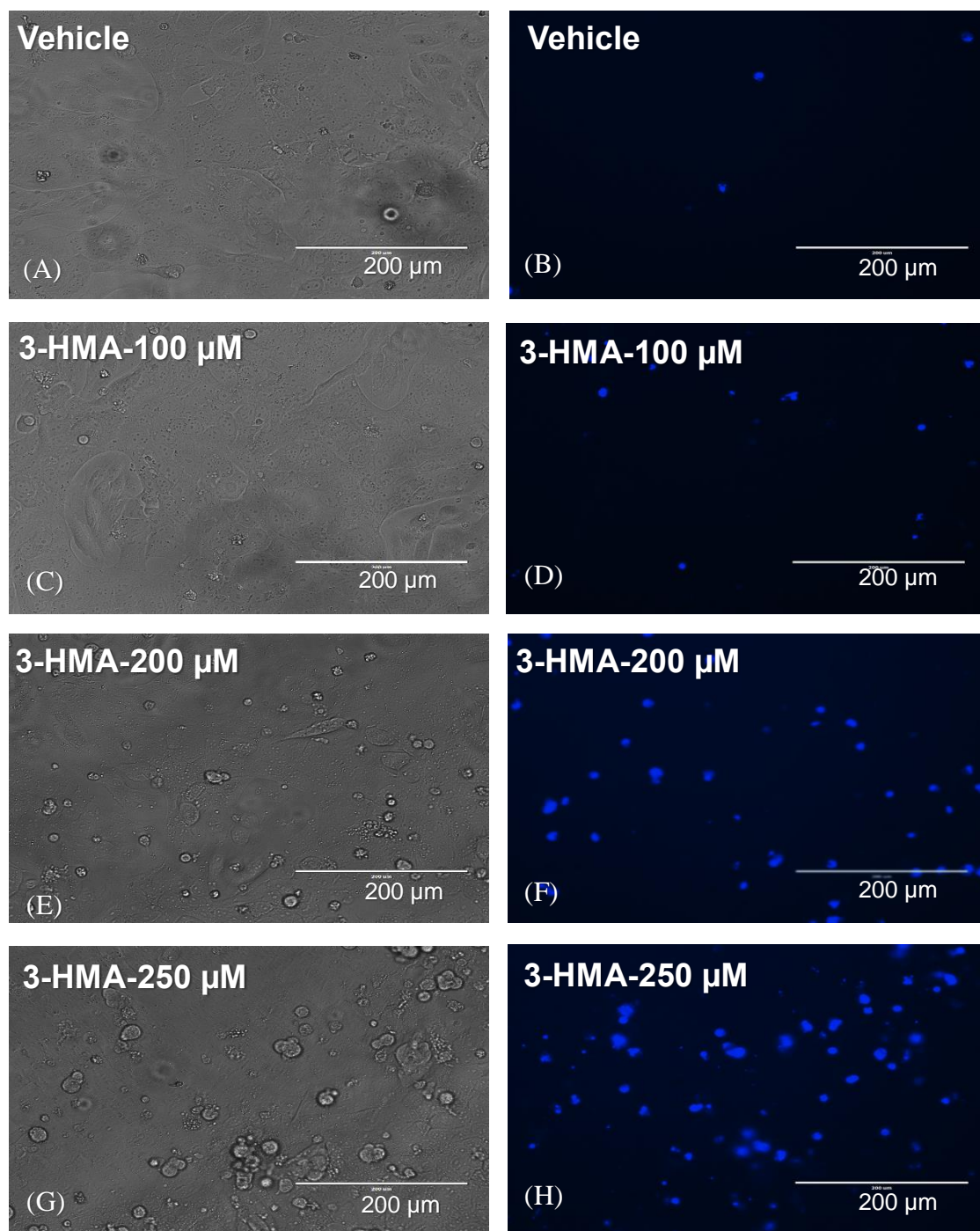
To examine whether treatment of 3-HFA to retinal cells induce lipoapoptosis; we assessed the biochemical characteristics nuclear morphological changes of lipoapoptosis using DNA-binding dye, 4', 6-diamidino-2-phenylindole (DAPI) and epifluorescence microscope. ARPE-19 cells treated with 3-HPA or 3-HMA showed increased characteristic nuclear morphological changes like nuclear fragmentation, pyknosis or chromatin condensation and cell shrinking compared to vehicle treated cells. The representative phase contrast image and DAPI stained fluorescent image of ARPE-19 cells treated with vehicle or 3-HPA (100-250  $\mu$ M) were showed in **Figure 7**. Representative images of retinal cells were with 3-HMA treatment (100-250  $\mu$ M) were showed in **Figure 8**. We observed an increase in DAPI staining with increasing concentration of 3-HPA (100-250  $\mu$ M) shown in **Figure 7 (C, D, E, F, G and H)** and with increasing concentration of 3-HMA compared to vehicle (100-250  $\mu$ M) suggesting retinal cell lipoapoptosis **Figure 8 (C, D, E, F, G and H)**. There was a significant increase in the percent apoptotic nuclei in 3-HPA or 3-HMA treated cells compared to vehicle **Figure 9 (A and B)**. Further, we measured caspase 3/7 activity by using fluorophore-tagged caspase substrate and expressed as fold change of caspase 3/7 activity over vehicle treatment. Treatment of 3-HPA or 3-HMA (250  $\mu$ M) significantly increased caspase 3/7 activity compared to vehicle treated cells **Figure 9 (C and D)**. These data suggest that 3-HFAs induces retinal pigment epithelial cell lipoapoptosis.

### **Evidence for cell death in ARPE-19 cells with 3-HFA treatment**

Another way to test cell death is by measuring nicotinamide adenine dinucleotide (NAD)-dependent cellular oxidoreductase enzymes. These enzymes reflect the metabolic activity of the cells and can reduce the tetrazolium dye, 3-(4,5-dimethylthiazol-2-yl)-2,5-diphenyltetrazolium bromide (MTT). We measured the MTT reduction and formazan formation as an indicator of cell survival in ARPE-19 cells with 3-HPA or 3-HMA treatment and expressed as percent cell survival. The 3-HMA (100-250  $\mu$ M) treated cells showed a significant decrease in percent cell survival compared to the vehicle treated cells shown in **Figure 9 (E)**. Also, treatment of 3-HPA (100-250  $\mu$ M) significantly decreased the percent cell survival in ARPE-19 cells compared to vehicle treated cells shown in **Figure 9 (F)**. The reduction in the cell survival with 3-HFA treatment was due to the toxic role of 3-HFA in altering mitochondrial functions. These data suggest that 3-HFA induces mitochondrial abnormalities and alters mitochondrial cellular and metabolic functions in ARPE-19 cells.



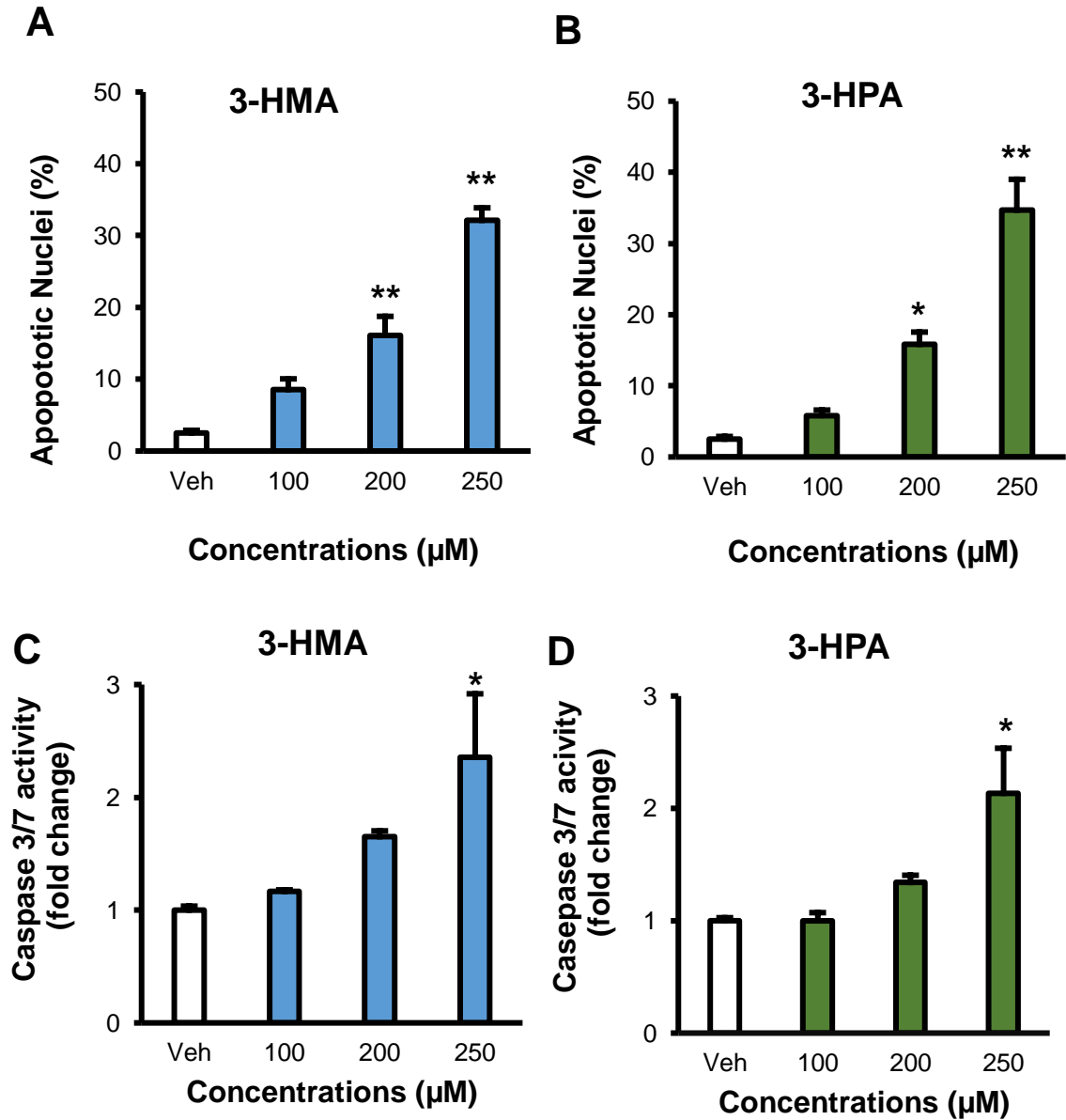
**Figure 7** Representative phase contrast and fluorescent DAPI stained live cell images of ARPE-19 cells with 3-HPA treatment. This representative figure shows that 3-hydroxy palmitic acids (3-HPA) induced nuclear morphological changes in retinal pigment epithelial cell (ARPE-19) lipoapoptosis. (A and B) are vehicle cells. (C-H) are ARPE-19 cells were treated with different concentrations of 3-HPA (100, 200, and 250 μM). Scale bar represents 200 μm.



**Figure 8** Representative phase contrast and fluorescent DAPI stained live cell images of ARPE-19 cells with 3-HMA treatment. This representative figure shows that 3-hydroxy myristic acids (3-HMA) nuclear morphological changes in in retinal pigment epithelial cell (ARPE-19) lipoapoptosis. (A and B)



are vehicle cells. (C-H) are ARPE-19 cells were treated with different concentrations of 3-HMA (100, 200, and 250  $\mu\text{M}$ ). Scale bar represents 200  $\mu\text{M}$ .



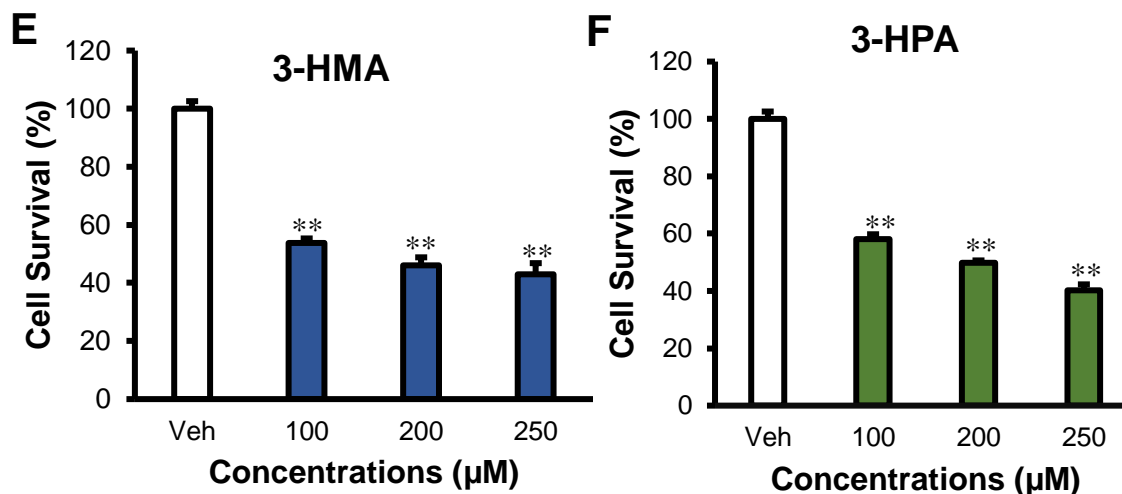


**Figure 9 Evidence for cell death in ARPE-19 cells with 3-HFA treatment. A)** Apoptotic nuclei percent for ARPE-10 cells treated with different concentrations of 3-hydroxy myristic acid (3-HMA) (100- 250 μM) and **B)** Cells treated with 3-hydroxy palmitic acid (3-HPA) (100-250 μM). **C)** Caspase 3/7 activity represented as fold change in ARPE-19 cells treated with 3-HMA **D)** cells treated with 3-HPA. **E and F)** Percent cell survival of ARPE-19 with different concentrations of 3-HMA or 3-HPA treatment. \* indicates P-value with different level of significance, \*(<0.05). \*\* (<0.01), and \*\*\*(<0.001). The differences in the apoptotic changes reached a statistical significance by obtaining that using ANOVA and Tukey test.

### **3.1.3 Saturated Free Fatty Palmitic Acid (PA) and Myristic Acid (MA) Did Not Induce Retinal Pigment Epithelial Cell Lipoapoptosis**

Similarly, ARPE-19 cells were treated with palmitic acid (PA) or myristic acid (MA) with different concentrations like 100, 150, 200 and 250 μM to emphasize the role of saturated free fatty acids in cell apoptosis. Treatment of PA or MA did not increase the percent retinal cell lipoapoptosis compared to vehicle treated cells shown in **Figure 10 and 11 (A, B, C, D, E, F, G, H, I, and J)**. The percent of apoptotic nuclei and caspase 3/7 activity did not show any difference in apoptosis in vehicle and retinal cells were treated with PA or MA

shown in **Figure 12 (A, B, C and D)**. Together, the treatment of saturated free fatty acids in retinal cells (ARPE-19) did not induce lipoapoptosis.

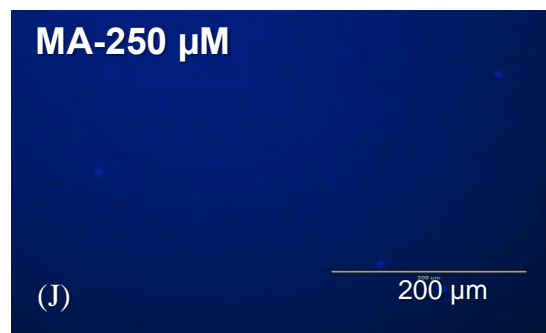
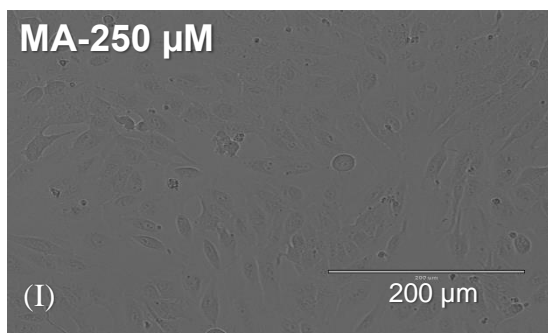
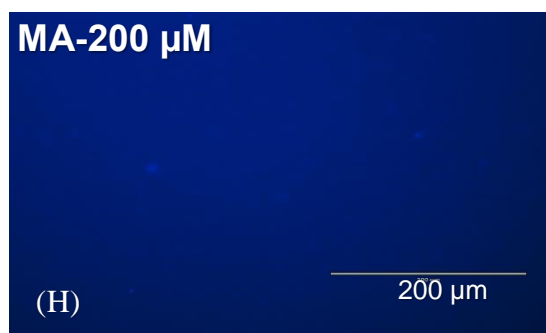
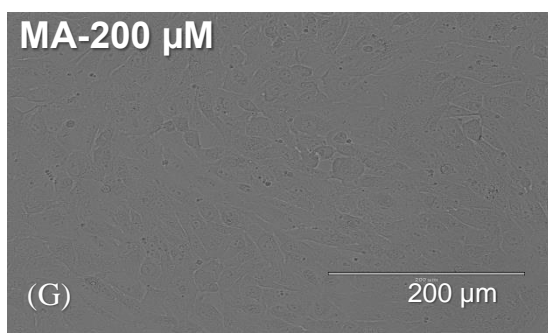
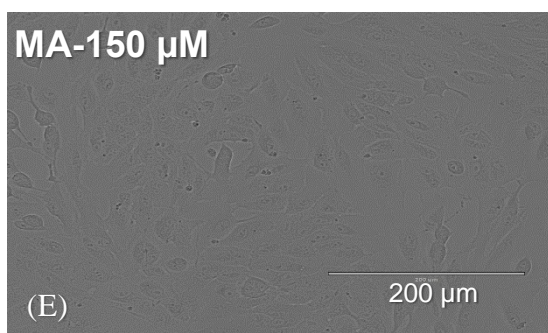
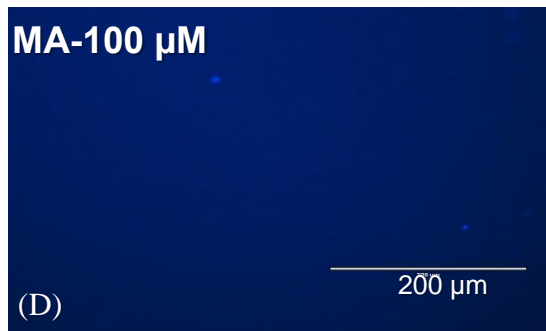
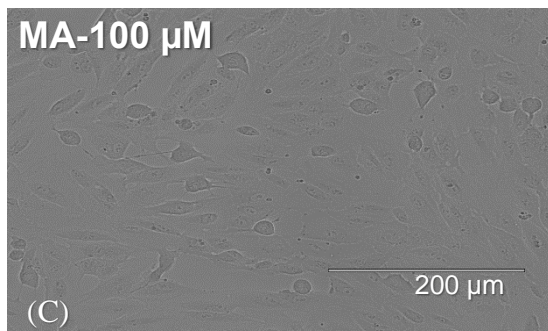
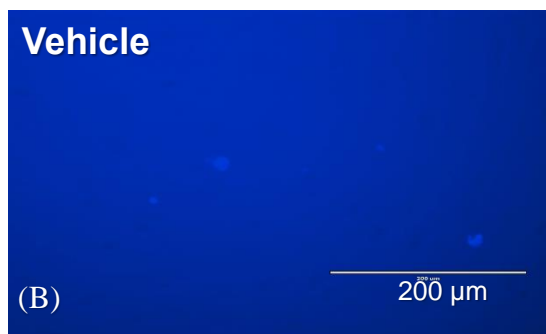
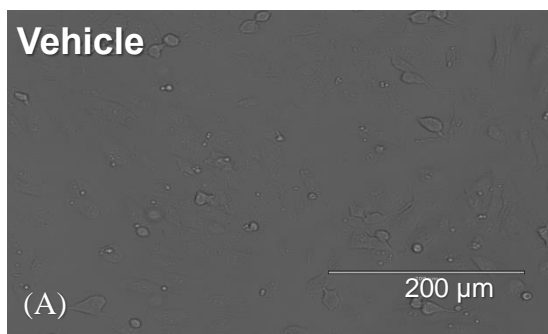


**Figure 10** Representative phase contrast and fluorescent DAPI stained live cell images of ARPE-19 cells with MA treatment. This representative figure shows that myristic acids (MA) did not increased staining of DAPI suggesting no change in characteristics of nuclear morphological changes in in retinal pigmented epithelial cell (ARPE-19) lipoapoptosis. **(A and B)** are vehicle cells. **(C, D, E, F, G, H, I and J)** ARPE-19 cells were treated with different concentrations of MA (100, 150, 200, and 250  $\mu$ M). Scale bar represents 200  $\mu$ M.

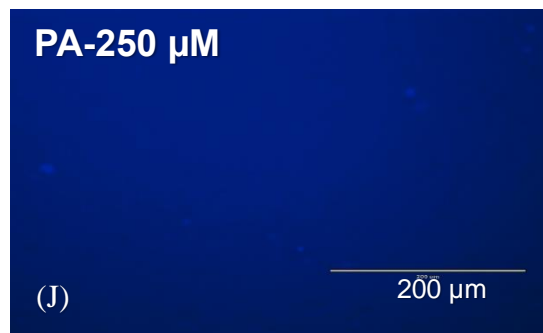
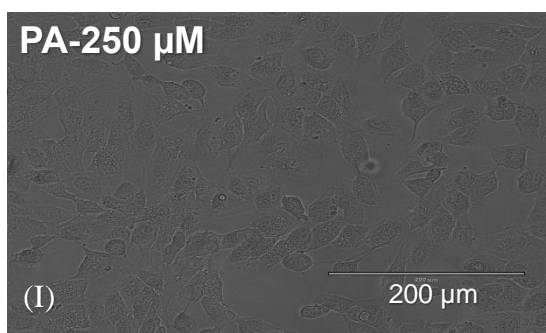
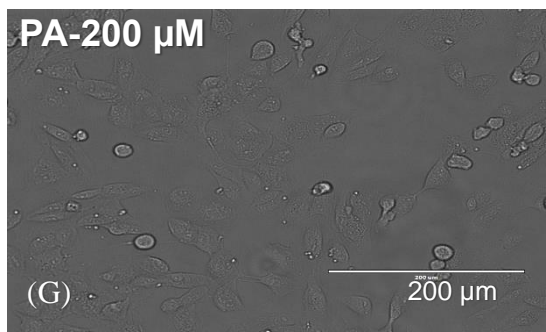
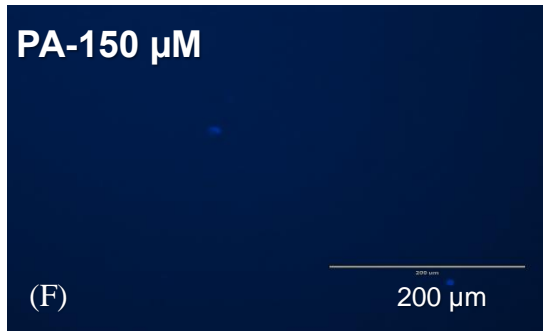
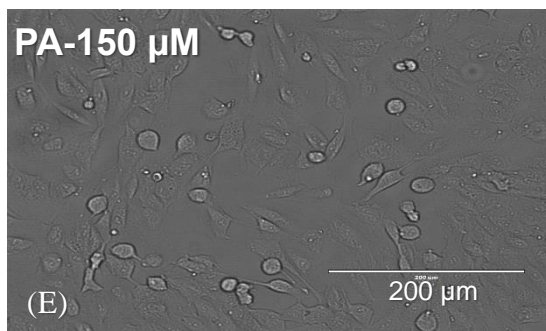
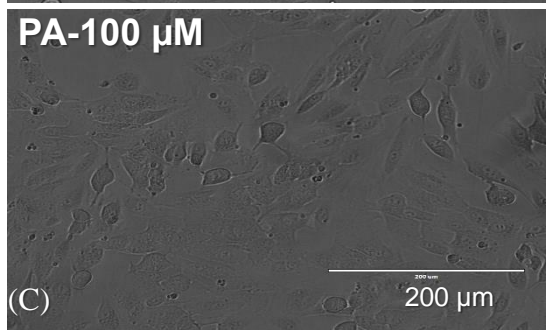
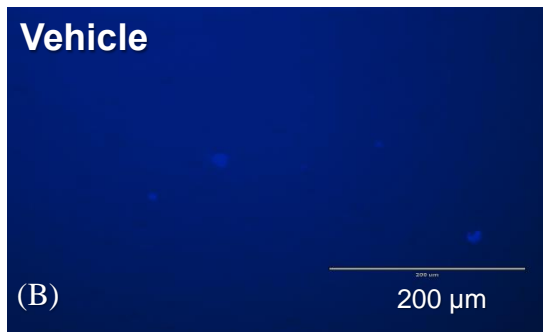
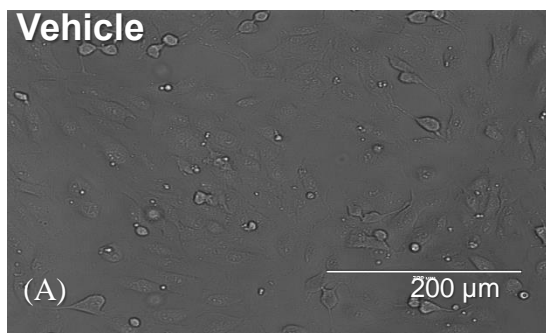


**Figure 11** Representative phase contrast and fluorescent DAPI stained live cell images of ARPE-19 cells with PA treatment. This representative images show that palmitic acids (PA) did not increase staining of DAPI suggesting no change in characteristics of nuclear morphological changes in in retinal pigment epithelial cell (ARPE-19) lipoapoptosis. **(A and B)** vehicle treated cells. **(C, D, E, f, G, H, I and J)** ARPE-19 cells were treated with different concentrations of PA (100, 150, 200, and 250  $\mu\text{M}$ ). Scale bar represents 200  $\mu\text{M}$ .

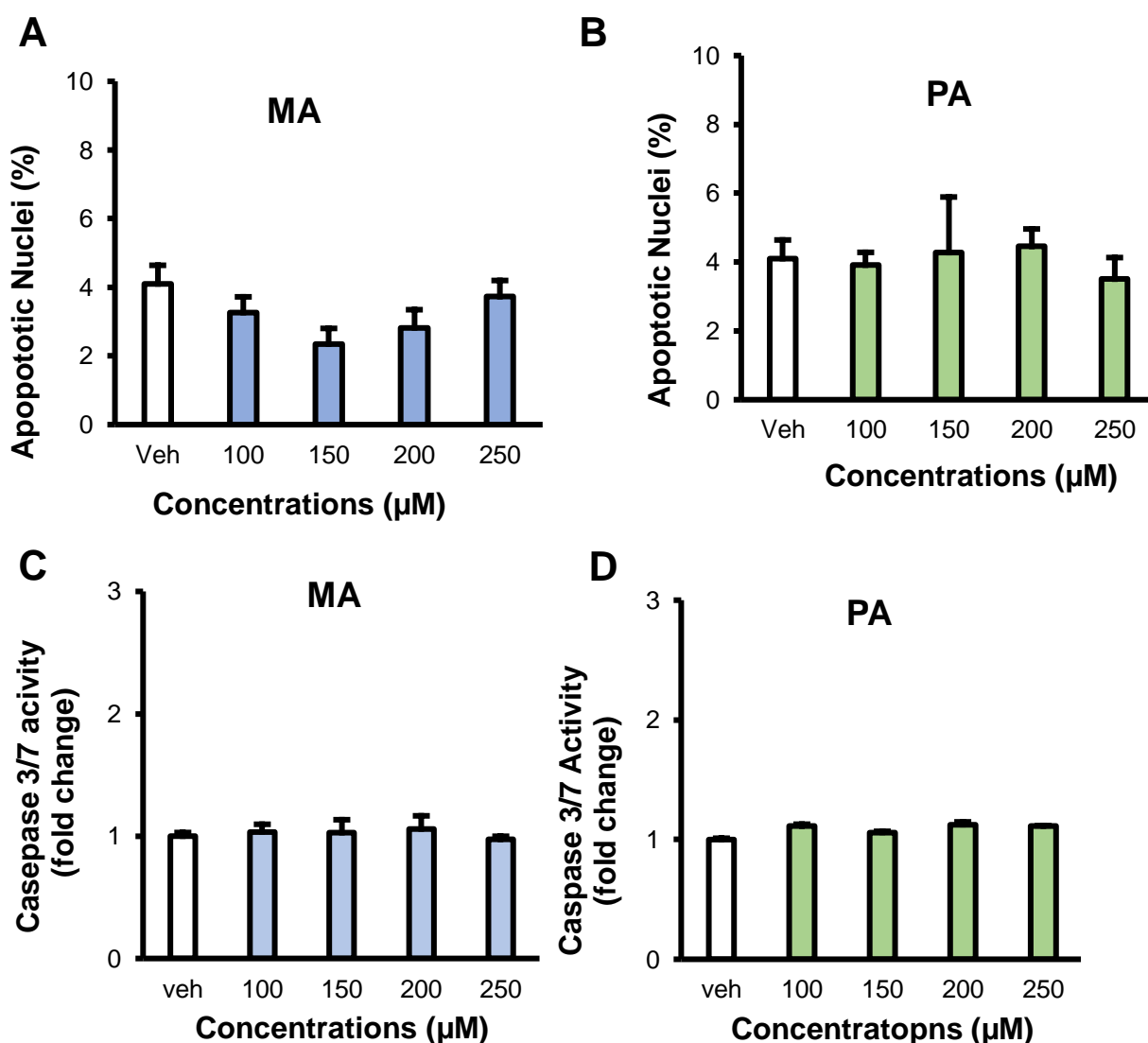


**Figure 12** Apoptotic nuclei percent for ARPE-10 cells treated with different concentrations of myristic acid (MA) (100-250  $\mu$ M) **(A)** and ARPE-19 cells treated with different concentrations of palmitic acid (PA) (100-250  $\mu$ M) **(B)**. Caspase 3/7 activity in ARPE-19 cells treated with MA **(C)** and PA **(D)**. \* indicates P-value with different level of significance, \*(<0.05). \*\* (<0.01), and \*\*\*(<0.001).

### **3.1.4 Biochemical Hallmark of Apoptosis**

Cell lysates of retinal cells treated with 3-HPA or 3-HMA were collected after 12, 18, and 24 hours of treatment. Western analysis showed that there was a dramatic increase in the expression of cleaved PARP in both 3-HMA and 3-HPA treated cells compared to vehicle treatment shown in **Figure 13**. Further, we observed that the levels of pro-apoptotic BH3 domain containing proteins, PUMA (p53 upregulated modulator of apoptosis) were upregulated after 12-24 hours of 3-HPA or 3-HMAs treatment in ARPE-19 cells. We have observed caspase 3/7 activation with 3-HPA or 3-HMA treatment in retinal cells.

Immunoblot analysis of active caspase 3 or cleaved-caspase 3 were increased in both 3-HMA and 3-HPA treated cells after 12-24 hours compared to vehicle treated retinal cells shown in **Figure 13**. Actin was used for control loading and showed no change among different time points of treatment and vehicle treated cells. These data suggest that the activation of pro-apoptotic proteins and the initiation of intrinsic pathway of apoptosis in 3-HPA or 3-HMA treated ARPE-19 cells.



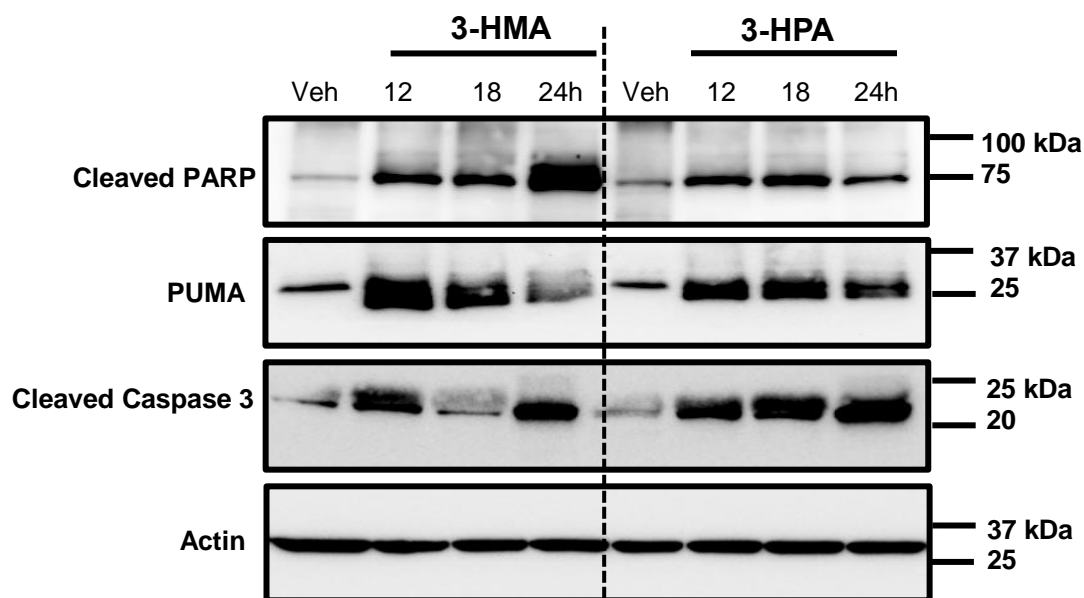
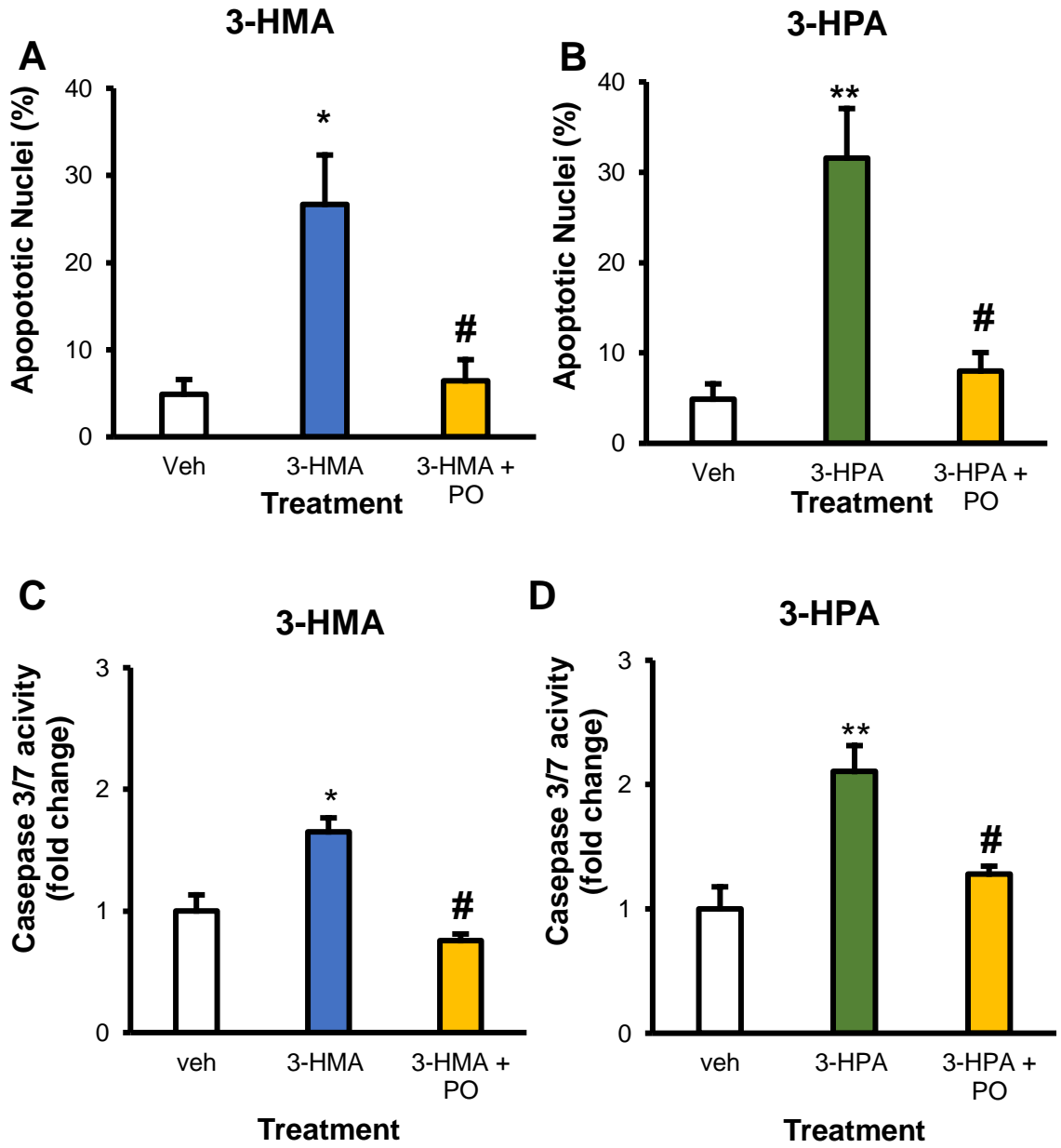


**Figure 13** Immunoblot analysis of Cleaved PARP, PUMA, Cleaved Caspase 3, and Actin in vehicle and 3-HPA/3-HMA treated ARPE-19 cells. Vehicle cells were isopropanol treatment and 3-HPA (250 μM) or 3-HMA (250 μM) treated cell lysates were analyzed after 12, 18, and 24 hours of treatment.

### 3.1.5 Palmitoleic Acid (PO) Protects Against 3-HFA-Induced Lipotoxicity

Palmitoleic acid (PO) is a mono-unsaturated omega-7 fatty acid and has been shown to be protective against free fatty acid-induced hepatocyte and cholangiocyte lipotoxicity (Yang, H., Miyahara, & Hatanaka, 2011); (Yang, Z. H. et al., 2011). To determine the beneficial role of PO in protecting ARPE-19 cells against the lipotoxicity, we co-treated 200 μM of PO with 3-HPA or 3-HMA for 24 hours. Similar to data presented in **Figure 9 (A and B)**, we observed that 3-HPA or 3-HMA increased percent apoptotic nuclei compared to vehicle treatment and the cotreatment of PO and 3-HPA or 3-HMA showed a dramatic decrease in percent apoptotic nuclei in retinal pigment epithelia cell shown in **Figure 14 (A**

**and B).** Similarly, cotreatment of PO and 3-HFA also reduced caspase 3/7 activity compared to cells treated with 3-HPA or 3-HMA alone shown in **Figure 14 (C and D)**. In addition, percent cell survival was significantly protected when ARPE-19 cells were co-treated with 3-HPA or 3-HMA with PO, compared to 3-HPA or 3-HMA alone, which decreases cell survival shown in **Figure 14 (E and F)**. These data suggest that PO protects against 3-HFA-induced retinal cell lipoapoptosis.



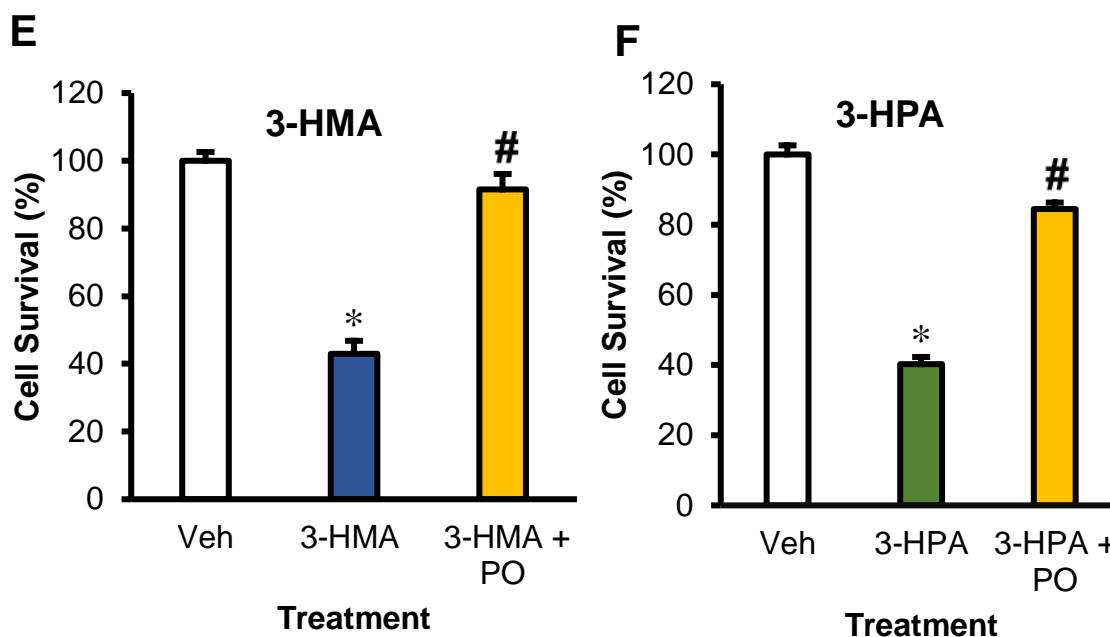


**Figure 14 Apoptotic cell death and caspase activation in ARPE-19 cells treated with 3-HPA or 3-HMA along with palmitoleate.** Apoptotic nuclei percent for ARPE-19 cells treated with 3-HMA and PO (**A**) and cells treated with 3-HPA and PO (**B**). Caspase 3/7 activation in ARPE-19 cells treated with 3-HMA and PO (**C**) and cells treated with 3-HPA and PO (**D**). Percent cell survival of ARPE-19 cells with 3-HMA (**E**) or 3-HPA (**F**) with and without palmitoleate (PO). Data represents mean  $\pm$  SEM from five independent experiments, n=5. \* indicates P-value with different level of significance of 3-HPA or 3-HMA compared to vehicle, \*(P<0.05). \*\* (P<0.01), and \*\*\*(P<0.001). #P>0.05 compared to 3-HPA or 3-HMA.

### 3.1.6 Retinal Cells Accumulate Lipid Droplets with 3-HPA or 3-HMA

#### Treatment

To investigate whether retinal cells accumulate lipid droplets, ARPE-19 cells were stained with oil red O' after cells were treated with 250  $\mu$ M of 3-HPA or 3-HMA for 24 hours with and without palmitoleate (PO). We observed that ARPE-19 cells with 3-HPA or 3-HMA treatment accumulated lipid droplets comparing to vehicle treated cells shown in **Figure 15**. The lipid droplets

accumulation is reduced in retinal cells co-treated with PO and 3-HPA or 3-HMA shown in **Figure 15**. We also quantitated Oil red O' staining in retinal cells with 3-HFA treatment by measure the absorbance of stained cells at 490 nm (Fei Z et al, 2011). ARPE-19 cells treated with 3-HPA or 3-HMA showed increased Oil red O staining and co-treatment of PO with 3-HPA or 3-HMA significantly reduced lipid accumulation in retinal cells shown in **Figure 16 (A and B)**. These data suggest that palmitoleate protects against 3-HFA-induced lipotoxicity in retinal cells by decreasing the accumulation of lipid droplets. Further studies are needed to elucidate the mechanism of PO preventing lipid droplet accumulation in retinal cells.

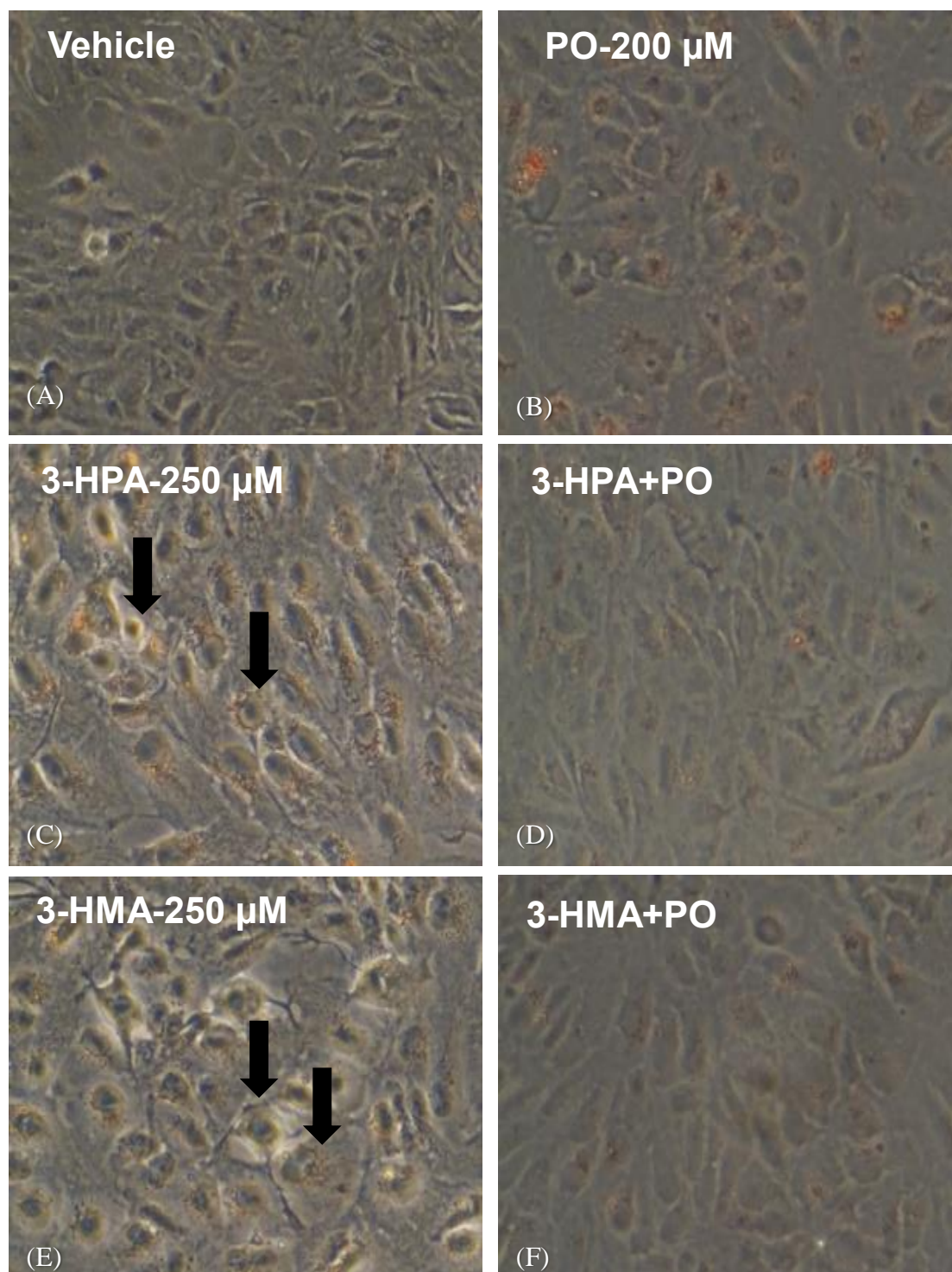


**Figure 15** Lipid droplet accumulation for ARPE-19 cells. Cells stained with Oil red O' assay visualized under light microscope. Control cells were treated with Vehicle (A) and Palmitoleate (B). Retinal cells with 250  $\mu$ M of 3-HMA (C) and 3-HPA treatment (E) for 24 hours showed increased Oil red 'O' staining. Co-treatment of palmitoleate (PO) with of 250  $\mu$ M 3-HPA or 3-HMA (D and F)

resulted in decreased Oil red 'O' staining. The images are representative images from three independent experiments, n=3.

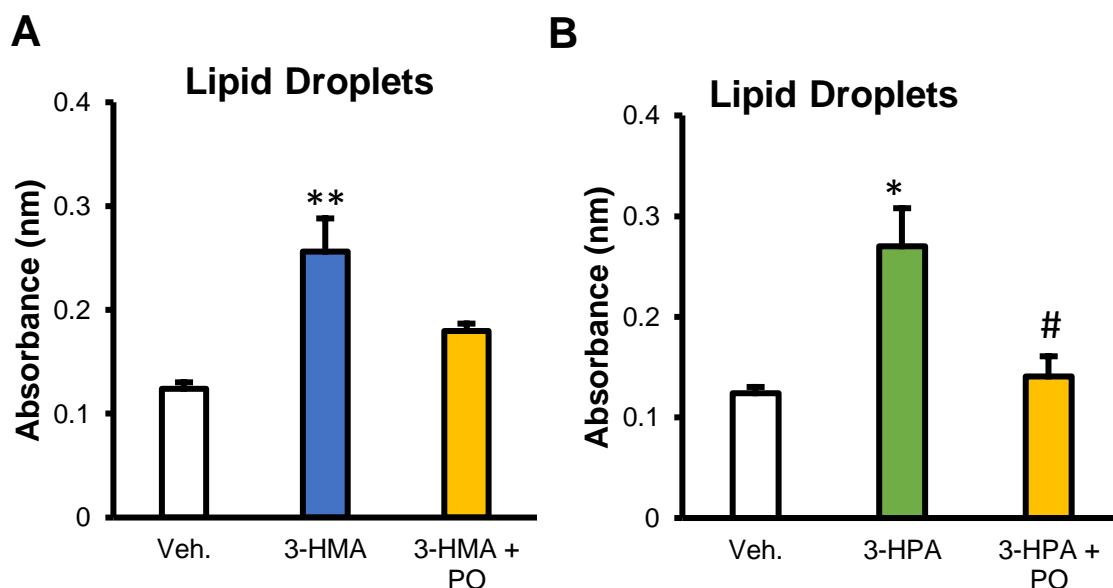


**Figure 16** Oil red O' assay absorbance in ARPE-19 cells. ARPE-19 cells treated with only 3-HMA (250  $\mu$ M) and both 3-HMA (250  $\mu$ M) and PO (200  $\mu$ M) (A). Cells treated with 3-HPA (250  $\mu$ M) alone and co-treated with 3-HPA (250  $\mu$ M) and PO (200  $\mu$ M) (B). \* indicates P-value with different level of significance of 3-HPA or 3-HMA compared to vehicle, \*(<0.05). \*\* (<0.01), and \*\*\*(<0.001). # indicates P-value for 3-HPA or 3-HMA with PO compared to 3-HPA or 3-HMA

### 3.1.7 3-HFA-Induces Retinal Cell lipoapoptosis is c-Jun N-terminal Kinase

#### Activation.

To determine the critical role of c-Jun N-terminal kinase (JNK) in 3-HFA-induced ARPE-19 lipoapoptosis; we used small molecule inhibitors of JNK (SP600125, JNKi). ARPE-19 cells were treated with 3-HPA or 3-HMA alone and co-treated with JNKi. First, we measured the activation of caspase in cells treated with only 3-HFAs and co-treatment of 3-HFAs with JNK inhibitor. Both 3-

HMA and 3-HPA treatment increases caspase 3/7 activation in retinal cells and co-treatment of 3-HFAs with SP600125 (JNK inhibitor) resulted in a significant protection against 3-HFAs induced caspase 3/7 activation **Figure 17 (A and B)**. Decreased percent cell survival of retinal cells with 3-HPA or 3-HMA treatment after 24 hours were significantly prevented with the cotreatment of JNK-i **Figure 17 (C and D)**.

### ***3.1.8 3-HFA Induces Retinal Cell Lipoapoptosis is Caspase Dependent***

To determine the critical role of caspase in 3-HFA-induced ARPE-19 lipoapoptosis; we used pan-caspase inhibitor (Z-VAD fmk). ARPE-19 cells were treated with 3-HPA or 3-HMA alone and co-treated with Z-VAD. First, we measured the activation of caspase in cells treated with only 3-HFAs and co-treatment of 3-HFAs with caspase inhibitor. We observed that co-treatment of 3-HFAs with Z-VAD-fmk decreased the 3-HFA-induced caspase activation in ARPE-19 cells **Figure 18 (A and B)**. Inhibition of caspase activity using Z-VAD also protected 3-HFA-induced apoptosis ARPE-19 cells as evidenced by an increase in percent cell survival with 3-HFA and Z-VAD co-treated retinal cells **Figure 18 (C and D)**.



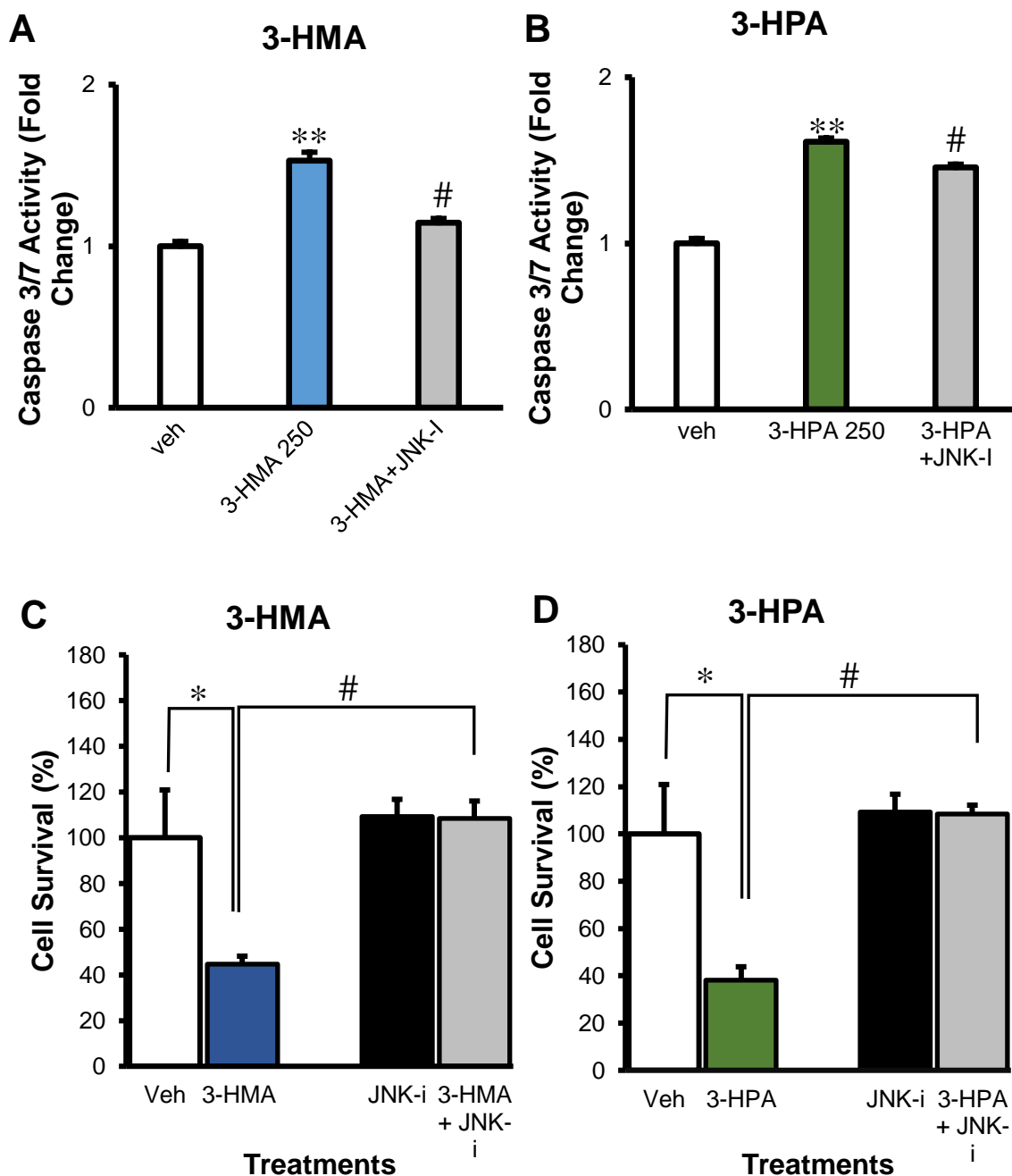


**Figure 17** Caspase 3/7 activity and percent cell survival in ARPE-19 cells treated with JNK-i. Caspase 3/7 activity were measured when cells were treated with 3-HMA and co-treated with 3-HMA and JNK inhibitor (SP600125, JNKi) (A) or treated with only 3-HPA or co-treated with 3-HPA and JNK-i. (B). Percent cell survival were measured when cells were treated with only 3-HMA or co-treated with 3-HMA JNKi (C) and only 3-HPA and co-treated with 3-HPA and JNKi (D). Data represent mean  $\pm$  SEM from five independent experiments, n=5. \*indicates

P-value with different level of significance of 3-HPA or 3-HMA compared to vehicle (veh), \*(<0.05), \*\* (<0.01), and \*\*\*(<0.001). # P<0.05 compared to 3-HMA or 3-HPA treatment

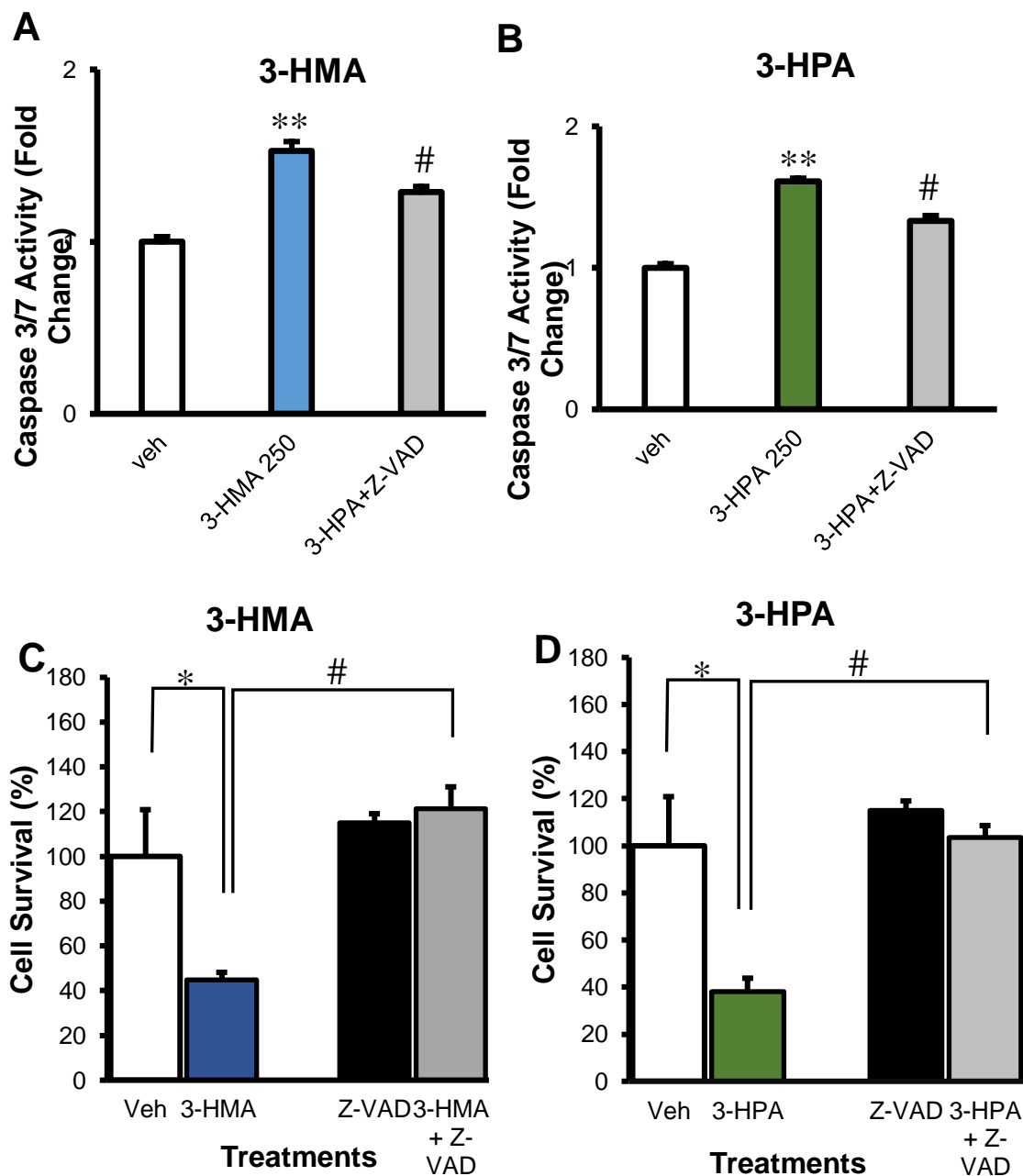


**Figure 18** Caspase 3/7 activity and percent cell survival in ARPE-19 cells treated with Z-VAD. Caspase 3/7 activity were measured when cells were treated with 3-HMA and co-treated with 3-HMA and caspase inhibitor (Z-VAD fmk) (A) or treated with only 3-HPA or co-treated with 3-HPA and Z-VAD (B). Percent cell survival were measured when cells were treated with only 3-HMA or

co-treated with 3-HMA Z-VAD (**C**) and only 3-HPA and co-treated with 3-HPA and Z-VAD (**D**). Data represent mean  $\pm$  SEM from five independent experiments, n=5. \*indicates P-value with different level of significance of 3-HPA or 3-HMA compared to vehicle (*veh*), \*(<0.05). \*\* (<0.01), and \*\*\*(<0.001). # P<0.05 compared to 3-HMA or 3-HPA treatment

## 4. CHAPTER IV: DISCUSSION, CONCLUSION, AND FUTURE DIRECTIONS

### 4.1 Discussion

This study confirms the lipotoxic role of 3-hydroxy fatty acids (3-HFAs) like 3-hydroxy palmitic acids (3-HPA) and 3-hydroxy myristic acids (3-HMA) in inducing lipoapoptosis in retinal pigmented epithelial cells (ARPE-19).

Accumulation of 3-HFAs are involved in children with LCHAD deficiency leading to develop pathophysiology such as retinopathy, cardiovascular disease, and muscle atrophy. Retinopathy is a widely associated with mitochondrial dysfunctions, however, there is a gap in knowledge on the mechanism of 3-HFA-induced retinal pigment epithelial cell lipotoxicity. The main goal of the present study is to test lipotoxicity in retinal cells and we used a normal human immortalized retinal pigmented epithelial cell, ARPE-19, *in vitro*. Lipoapoptosis is known as programmed cell death that is caused due to the exposure of high concentration of fatty acids. Apoptosis due to caspase activation and mitochondrial alteration, which are characterized by oxidative stress due to accumulating toxic free fatty acids in the circulation during obesity and metabolic syndrome has been well established (Wajner & Umpierrez, 2016) . We characterized retinal pigmented epithelial cell features and evaluated caspases activity, mitochondrial functions, lipid droplets, and biochemical hallmarks of apoptosis with 3-HFA exposure. To examine all these characteristics, cells were treated with 3-HFAs including 3-hydroxy palmitic acids (3-HPA) or 3-hydroxy

myristic acids (3-HMA) to mimic and simulate pathophysiological condition in LCHAD patient's blood circulation. Patients with defective fatty acid oxidation metabolism especially who are deficient in the enzyme long-chain hydroxy acyl-CoA dehydrogenase (LCHAD), can accumulate metabolites and substrates such as saturated free fatty acids and hydroxy fatty acids. Here we hypothesize that the retinal cell apoptosis could contribute and result in retinopathy observed in LCHAD deficient patient. In the present study, we demonstrated that 3-HPA or 3-HMA exposure to retinal pigment epithelial cells resulted in retinal cell lipoapoptosis. Apoptosis can leads to mitochondrial stress, caspases activation, and lipid accumulation.

Lipotoxic role of 3-HFAs in inducing lipoapoptosis is in agreement with our unpublished work that has shown the accumulation of 3-HFAs including 3-HMA or 3-HPA induces hepatocyte lipoapoptosis leading to apoptosis and caspase activation (Natarajan, S. K. & Ibdah, 2018). Additionally, previous study conducted on human disease model created from a pluripotent stem cell (hiPSC) differentiation to retinal cells demonstrates that retinal pigmented epithelial cells developed pathogenic changes with retinal characteristics and nuclear morphology suggesting the apoptosis (Padmini et al., 2015).

Mitochondria are the major site for energy metabolism and mitochondrial mediated activation of intrinsic pathway of apoptosis is characterized with mitochondrial permeabilization and release of cytochrome C resulting in the formation of apoptosome and activation of caspases (Natarajan SK, 17 February 2012) . Our previous research using placenta from patients with acute fatty liver

of pregnancy (AFLP) showed oxidative stress in the placental subcellular organelle and maternal systemic (Natarajan, S. et al., 2010; Natarajan, S., Thangaraj, Eapen, Ramachandran, & Balasubramanian, 2011; Natarajan, S. K., Eapen, Pullimood, & Balasubramanian, 2006) . Defects in placental mitochondrial fatty acid oxidation can channel the fatty acids to peroxisomal  $\beta$ -oxidation and microsomal omega-oxidation. Increased peroxisomal  $\beta$ -oxidation would result in the generation of hydrogen peroxide, which could: 1) damage subcellular organelles; 2) alter redox homeostasis; 3) damage cellular redox-sensitive protein function; and 4) contribute to the cell death and disease development. Further, placental mitochondria isolated from patients with AFLP showed mitochondrial dysfunction and the levels of antioxidants such as tocopherol and retinol were decreased in the systemic circulation of AFLP patients compared to controls suggesting oxidative stress in maternal systemic circulation in patients with AFLP. Further, we have shown animals treated with valproate, an inhibitor of liver mitochondrial  $\beta$ -oxidation, showed hepatic mitochondrial dysfunction, oxidative stress and microvesicular steatosis in the liver suggesting that a blockage in mitochondrial  $\beta$ -oxidation would induce hepatic mitochondrial dysfunction and oxidative stress in the liver (Natarajan, S. et al., 2010; Natarajan, S. et al., 2011; Natarajan, S. K. et al., 2006). Similar to the placental and liver cells; in the present work retinal cells exposed to 3-HPA resulted significant alteration in the mitochondrial bioenergetics and functions. Mitochondrial dysfunction and damage results in alteration to mitochondrial respiration with the exposure of lipotoxic 3-HFA metabolites. In ARPE-19 cells

that were treated with 3-HPA, there was a significant decrease in the ATP production, basal respiration and spare respiratory capacity, and coupling efficiency. All these abnormalities resulted to compensate the stress that was induced by the accumulation of 3-HFA. The findings suggest that mitochondrial stress is the mechanism that contributes to the 3-HFA-induced ARPE-19 cell death. Similar to our findings, a recent study showed that defective mitochondria resulted in altering the respiratory chain and coupling efficiency which increase reactive oxygen species (ROS) (Radek, Marco, & Heinz, 2014).

Retinal pigment epithelial cells (RPE) functions to maintain recycling of 11-cis-retinaldehyde, absorbs excess light and contributes to the phagocytosis of photoreceptors fragments (Tivadar O., Palczewska G., Palczewski K., 2011 May 12). RPE cells also store retinyl esters in retinosomes and excess fatty acids as lipid droplets (Brink. D. et al., 2018). Lipid droplets accumulation in RPE can impair normal cell signaling leading to cellular dysfunction and apoptotic cell death (Meyer et al., 2011). Similarly, ARPE-19 cells have been shown to accumulate lipid droplets (Chena et al., 2019) . It has also been shown that retinal cells can accumulate lipid droplets during LCHAD deficiency (Chena et al., 2019) Further free fatty acid and high glyucose exposure during obesity and metabolic syndrome has also been shown to increased lipids droplets accumulation in retinal pigment epithelial cells (Chena *et al.*, 2019). The retinal dysfunction due to free fatty acid and high glucose exposure to retinal cells has been demonstrated as the mechanism for the progression of diabetic retinopathy which resulted in retinal atrophy (Chena et al., 2019). Rudolf *et al.*, showed that

retinal pigment epithelial cells can also accumulate lipid droplets with aging in human retina through accumulations of lipoproteins particles resulting in age-related macular degeneration (Rudolf & Curcio, 2009). Further, it has been shown that overexpression of fatty acid transport protein (FATP) in retinal cells of *Drosophila* and mice enhanced lipid droplets accumulation (Brink. D. et al., 2018). Under normal conditions, these lipid droplets have a beneficial effect on the retinal cells and photoreceptors. However, under vitamin A deficiency diet, the accumulation lipids droplets were toxic which disturbed the photoreceptors homeostasis (Van Den et al., 2018).

Our lab has previously shown that forkhead family of transcription factor class O3 (FoxO3) is activated in hepatocytes that were treated with 3-HFAs (Natarajan, S. K. et al., 2017) . The activation of FoxO3 is associated with cell death signaling, because FoxO3 can transcriptionally upregulates the pro-apoptotic protein, like BIM, PUMA and NoxA which can induce lipoapoptosis (Natarajan, S. K. et al., 2017). In the present study, we observed biochemical evidence of apoptosis such as increased levels of PUMA in ARPE-19 cells treated with 3-HPA or 3-HMA. However, the role of FoxO3 activation and the critical role of pro-apoptotic protein, PUMA in retinal lipoapoptosis requires further investigation. The increased expression of pro-apoptotic BH<sub>3</sub> domain containing protein, PUMA indicates the activation of intrinsic pathway of apoptosis. Increased levels of PUMA can act against anti-apoptotic proteins like BCL2 and MCL1. The expression of anti-apoptotic proteins in retinal pigment epithelial cells with 3-HFAs requires further investigation. Caspase 3/7 enzyme



activity is responsible for cleaving downstream caspase substrates such as poly adenosine-ribose polymerase (PARP). The increased levels of caspase substrate, cleaved PARP and cleaved caspase 3, are key markers for the late phase of the apoptosis were evident in retinal cells exposure to 3-HFA. In addition to caspase substrate, inhibition of caspases using small molecular inhibitor blocked 3-HFA-induced lipoapoptosis in retinal cells suggestions the critical role of caspase activation during retinal pigment cell lipoapoptosis. In summary, apoptotic hallmarks were evident when ARPE-19 cells were exposed to higher concentrations of 3-HPA or 3-HMA, suggesting the involvement of retinal cell lipoapoptosis in the development of retinopathy in patients with LCHAD deficiency.

In the present study, we proposed a dietary nutrient intervention to protect against 3-HFA-induced lipotoxicity in retinal cells with palmitoleic acid (PO) supplementation. PO is an omega 7-mono unsaturated fatty acids and PO has been shown to protect against saturated free fatty acid-induced hepatocyte and cholangiocyte lipoapoptosis (Akazawa, 2010). PO treatment has been shown to abolish palmitate-induced endoplasmic reticulum (ER) stress response, JNK activation, mitochondrial pro-apoptotic mediators, and lipotoxicity (Akazawa, 2010) . Further, supplementation of palmitoleate has been shown to unalter the expression of stearoyl CoA-desaturase1 (SCD1), an enzyme that can convert palmitate into palmitoleate, however palmitoleate (PO) increased lipid droplets accumulation and decreases the lipotoxicity of saturated FFAs in hepatocytes (Akazawa, 2010) . In addition, decreased expression of SCD1 were found to

enhance palmitate-induced trophoblast lipotoxicity (Yang, C., Lim, Bazer, & Song, 2018). Nevertheless, the *in vivo* effect of PO on retinopathy still needed to be elucidated. PO is involved in many processes associated with cell function, acts as anti-apoptotic fatty acid, and improves lipid profile in obese mice (Yang, H., Miyahara, & Hatanaka, 2011). Further, supplementation of PO significantly reduces the hepatic triglyceride levels and lipid droplets accumulation in the liver of diabetic mice (Yang, H. et al., 2011). In the present study, our data demonstrated the positive role of PO in protecting against lipoapoptosis. Additionally, lipid droplets accumulation in ARPE-19 has been decreased significantly when cells treated with PO compared to 3-HFAs treatment. Also, palmitoleate protects against 3-HFA-induced retinal cell lipoapoptosis. We observed that treatment of JNK-inhibitor protected against 3-HFA induced retinal lipoapoptosis, these data suggest that JNK plays a critical role in retinal lipoapoptosis. Saturated free fatty acids are known to active JNK-dependent hepatocyte lipoapoptosis (Malhi. H., Bronk. S., Werneburg. N., and Gores. G., 2006). However, our lab has previously showed that JNK is not critical for cholangiocyte lipoapoptosis (Natarajan, S. K. et al., 2014). Here, we speculate that PO protection could involve prevention of JNK activation, further studies are needed to demonstrate the role of JNK signaling with PO supplementation. Chen et al., showed that JNK could transitionary upregulates the expression of PUMA protein during cell death process (Chena et al., 2019). However, it is still not clear whether treatment with PO could alter the transcriptional activity of JNK for the protection against retinal lipoapoptosis and requires further investigation.

Further, demonstrating the retinal cell lipoapoptosis in animal models of LCHAD deficiency and dietary supplementation of palmitoleate protecting against retinal injury, retinopathy and lipoapoptosis requires further investigation.

#### **4.2 Conclusions and Future Directions**

In conclusion, the data from the present study show that 3-hydroxy fatty acids can induce lipoapoptosis in retinal pigment epithelial cells. The mechanisms are involved in lipoapoptosis were; caspase 3/7 activation, mitochondrial dysfunction, and activation of pro-apoptotic protein PUMA. All these events together support the hypothesis that 3-HFA induces lipotoxicity in retinal cells *in vitro*. Also, we show evidence for palmitoleate protection against 3-HFA induced lipotoxicity. The data presented in this study were from ARPE-19 cell line. Our next steps are to use LCHAD knockdown animal and confirm the lipotoxic role of 3-hydroxy fatty acids in inducing the retinal damage and retinopathy. In addition, we would also like to use CRISPR/Cas9 system to introduce pathogenic mutation in LCHAD encoding gene, *HADHA in retinal cells* to test retinal cell lipoapoptosis. Further investigations are also required to understand the mechanism of PO in protecting against 3-HFA-induced retinal cell lipotoxicity.

## References

1. Agilent Technologies. (2017). Agilent seahorse XF cell mito stress test kit . *Agilent Technologies, Inc, 100*(103015)
2. Agilent Technologies. (2018). *Cell characterization: The XFe24/XF24 analyzer and the cell energy phenotype test.* ( No. 5991-8640EN). USA: Agilent Technologies, Inc.
3. Akazawa, Y. (2010). Palmitoleate attenuates palmitate-induced bim and PUMA up-regulation and hepatocyte lipopoptosis. *J Hepatol, 52*, 586-593.
4. Blagosklonny, M. V. (2008). Aging: ROS or TOR. *Cell Cycle, 7*(21), 3344-3354. doi:10.4161/cc.7.21.6965
5. Brink, D. et al.,. (2018). Expression of fatty acid transport protein in retinal pigment cells promotes lipid droplet expansion and photoreceptor homeostasis . *PLoS Genetics,*
6. Chena, Q., Tangb, L., Xina, G., Li, S., Ma, L., Xu, Y., . . . Huang, Z. (2019). Oxidative stress mediated by lipid metabolism contributes to high glucose-induced senescence in retinal pigment epithelium. *Free Radical Biology and Medicine 48-58, 130*, 48-58.
7. Den, B. M. E., Wanders, R. J., Morris, A. A., Lodewijk, I. J., Heymans, H. S., & Wijburg, F. A. (2002). Long-chain 3-hydroxyacyl-CoA dehydrogenase deficiency: Clinical presentation and follow-up 50 patients. *Pediatrics, 109*(1), 99-104.

8. Derks, T. G., Touw, C. M., Ribas, G. S., Biancini, G. B., Vanzin, C. S., Negretto, G., . . . Vargas, C. R. (2014). Experimental evidence for protein oxidative damage and altered antioxidant defense in patients with medium-chain acyl-CoA dehydrogenase deficiency. *Journal of Inherited Metabolic Disease*, *37*, 783-789.
9. Enns, G. M., Bennett, M. J., Hoppel, C. L., Goodman, S. I., Weisiger, K., Ohnstad, C. I., . . . Packman, S. (2000). Mitochondrial respiratory chain complex I deficiency with clinical and biochemical features of long-chain 3-hydroxyacyl-coenzyme A dehydrogenase deficiency. *Journal of Pediatrics*, *136*, 251-254.
10. Fei Z et al. (2011). *Ankrd26* gene disruption enhances adipogenesis of mouse embryonic fibroblasts. *Jbc*, *280*(31) doi:27761-27768
11. Feillet, F., Steinmann, G., Vianey-Saban, C., de Chillou, C., Sadoul, N., Lefebvre, E., . . . Bollaert, P. E. (2003). Adult presentation of MCAD deficiency revealed by coma and severe arrhythmias. *Intensive Care Medicine Journal*, *29*, 1594-1597.
12. Friedman, J. R., & Jodi, N. (2014). Mitochondrial form and function. *Nature Journal*, *505*(7483), 335-343.
13. Gavrieli, Y., Sherman, Y., & Ben-Sasson, S. (1992). Identification of programmed cell death in situ via specific labelling of nuclear DNA fragmentation. *Journal of Cell Biology*, *119*, 493-501.
14. Gillingham, M., Weleber, R., & Neuringer, M. (2005). Effect of optimal dietary therapy upon visual function in children with long-chain 3-hydroxyacyl CoA

- dehydrogenase and trifunctional protein deficiency. *Molecular Genetics and Metabolism Journal*, 86, 124-133.
15. Gillingham, M., Scott, B., Elliott, D., & Harding, C. (2006). Metabolic control during exercise with and without medium-chain triglycerides (MCT) in children with long-chain 3-hydroxy acyl-CoA dehydrogenase (LCHAD) or trifunctional protein (TFP) deficiency. *Molecular Genetics and Metabolism Journal*, 89, 58-63.
16. Hagenfeldt, L., Venizelos, N., & Von Döbeln, U. (1995). Clinical and biochemical presentation of long-chain 3-hydroxyacyl-CoA dehydrogenase deficiency. *Journal of Inherited Metabolic Disease*, 18, 245-248.
17. He, F. (2011). BCA (bicinchoninic acid) protein assay. bio-protocol Bio101.44 doi:10.21769/BioProtoc.44.
18. Hickmann, F. H., Cecatto, C., Kleemann, D., Monteiro, W. O., Castilho, R. F., Amaral, A. U., & Wajner, M. (2015). Uncoupling, metabolic inhibition and induction of mitochondrial permeability transition in rat liver mitochondria caused by the major long-chain hydroxyl monocarboxylic fatty acids accumulating in LCHAD deficiency. *Biochimica Et Biophysica Acta*, 1847, 620-628.
19. Jones, P., Moffitt, M., Joseph, D., Harthcock, P., Boriack, R., Ibdah, J., . . . Bennett, M. (2001). Accumulation of free 3-hydroxy fatty acids in the culture media of fibroblasts from patients deficient in long-chain l-3-hydroxyacyl-CoA dehydrogenase: A useful diagnostic aid. *Clinical Chemist*, 47, 1190-1194.

20. Jones, P., Quinn, R., Fennessey, P., Tjoa, S., Goodman, S., Fiore, S., . . . Bennett, M. (2000). Improved stable isotope dilution-gas chromatography-mass spectrometry method for serum or plasma free 3-hydroxy- fatty acids and its utility for the study of disorders of mitochondrial fatty acid beta-oxidation. *Clinical Chemist*, *46*, 149-155.
21. Kalkavan, H., & Douglas, R. G. (2017). MOMP, cell suicide as a BCL-2 family business . *Cell Death and Differentiation*, *25*(1), 46-55.  
doi:10.1038/cdd.2017.179.
22. Kinman, R. P., Kasumov, T., Jobbins, K. A., Thomas, K. R., Adams, J. E., Brunengraber, L. N., . . . Brunengraber, H. (2006). Parenteral and enteral metabolism of anaplerotic triheptanoin in normal rats. *American Journal of Physiology-Endocrinology and Metabolism*, *291*, 860-866.
23. Kroemer, G., Galluzzi, L., Vandenabeele, P., Abrams, J., Alnemri, E., Baehrecke, E., . . . Melino, G. (2009). Classification of cell death: Recommendations of the nomenclature committee on cell death. *Cell Death & Differentiation Journal*, *16*, 3-11.
24. Lindner, M., Gramer, G., Haege, G., Fang-Hoffmann, J., Schwab, K. O., Tacke, U., . . . Hoffmann, G. F. (2011). Efficacy and outcome of expanded newborn screening for metabolic diseases report of 10 years from south-west germany. *Orphanet Journal of Rare Diseases*, *6*(44), 1-10.  
doi:10.1186/1750-1172-6-44
25. Malhi. H., Bronk. S., Werneburg. N., and Gores. G. (2006). Free fatty acids induce JNK-dependent hepatocyte lipoapoptosis. *Jbc*,

26. Meerloo, J. v., Kaspers, G. J. L., & Cloos, J. (2011). Cell sensitivity assays: The MTT assay." cancer cell culture: Methods and protocols . In I. A. Cree (Ed.), (2nd ed., pp. 237-245) Springer Science+Business Media, LLC.
27. Merritt, J. L., Norris, M., & Kanungo, S. ((2018)). Fatty acid oxidation disorders . *Annals of Translational Medicine*, 6(24), 473. doi:10.21037/atm.2018.10.57
28. Meyer, J., Howden, S., Wallace, K., Verhoeven, A., Wright, L., Capowski, E., . . . Gamm, D. (2011). Optic vesicle-like structures derived from human pluripotent stem cells facilitate a customized approach to retinal disease treatment. *Stem Cells*, 1206(18) doi:10.1002/stem.674
29. Morgan, N., & Dhayal, S. (2010). Unsaturated fatty acids as cytoprotective agents in the pancreatic beta-cell. *Prostaglandins Leukot Essent Fatty Acids*, 82, 231-236.
30. Morgan, N., Dhayal, S., Diakogiannaki, E., & Welters, H. (2008). Unsaturated fatty acids as cytoprotective agents in the pancreatic beta-cell. *Biochemical Society Transactions*, 36, 905-908.
31. Najdekr, L., Gardlo, A., Madrova, L., Friedecky, D., Janeckova, H., Correa, E. S., . . . Adam, T. (2015). Oxidized phosphatidylcholines suggest oxidative stress in patients with medium-chain acyl-CoA dehydrogenase deficiency. *Talanta*, 139, 62-66.
32. Natarajan SK, B. D. (17 February 2012). Role of apoptosis-inducing factor, proline dehydrogenase, and NADPH oxidase in apoptosis and oxidative



stress. *Cell Health and Cytoskeletal*, 4, 11-27.

doi:<https://doi.org/10.2147/CHC.S4955>

33. Natarajan, S., Thangaraj, R., Eapen, E., Ramachandran, A., & Balasubramanian, A. (2011). Acute fatty liver of pregnancy: An update on mechanism. *Obstetric Medicine*, 4, 99-103.
34. Natarajan, S., Thangaraj, R., null, Ramachandran, Mukhopadhyaya, A., Mathai, M., . . . Balasubramanian, A. (2010). Liver injury in acute fatty liver of pregnancy: Possible link to placental mitochondrial dysfunction and oxidative stress. *Hepatology*, 51(1), 191-200. doi:10.1002/hep.23245.
35. Natarajan, S. K., Eapen, C., Pullimood, A., & Balasubramanian, K. (2006). Oxidative stress in experimental liver microvesicular steatosis: Role of mitochondria and peroxisomes. *Hepatology*, 42(8), 1240-1249.
36. Natarajan, S. K., & Ibdah, J. A. (2018). Role of 3-hydroxy fatty acid-induced hepatic lipotoxicity in acute fatty liver of pregnancy. *International Journal of Molecular Sciences*, 19(322), 1-17.
37. Natarajan, S. K., Ingham, S. A., Mohr, A. M., Wehrkamp, C. J., Ray, A., Roy, S., . . . Mott, J. L. (2014). Saturated free fatty acids induce cholangiocyte lipoapoptosis. *Hepatology*, 60, 1942-1956.
38. Natarajan, S. K., Stringham, B. A., Mohr, A. M., Wehrkamp, C. J., Lu, S., Phillippi, M. A., . . . Mott, J. L. (2017). FoxO3 increases miR-34a to cause palmitate-induced cholangiocyte lipoapoptosis. *Journal of Lipid Research*, 58, 866-875.

39. Olpin, S. E. (2013). Pathophysiology of fatty acid oxidation disorders and resultant phenotypic variability. *Journal of Inherited Metabolic Disease*, *36*, 2013-645. doi:658
40. Padmini, P. P., Tanja, I., Ras, T., Tuulia, H., Timo, O., Anu, S., . . . Tiina, T. (2015). Patient-specific induced pluripotent stem Cell-Derived RPE cells: Understanding the pathogenesis of retinopathy in long-chain 3-hydroxyacyl-CoA dehydrogenase deficiency. *Investigative Ophthalmology and Visual Science, the Association for Research in Vision and Ophthalmology*, *56*(5), 3371. doi:10.1167/iovs.14-14007
41. Parker, J., W., D., Haas, R., Stumpf, D. A., & Eguren, L. A. (1983). Effects of octanoate on rat brain and liver mitochondria. *Neurology*, *33*, 1374-1377.
42. Promega. (TB323). Caspase-glo® 3/7 assay. *Tb323*,
43. Radek, S., Marco, N., & Heinz, D. O. (2014). Control of mitochondrial integrity in ageing and disease” philosophical transactions of the royal society of london. *Series B, Biological Sciences*, *369*(1646), 1-18. doi:10.1098/rstb.2013.0439
44. Rocchiccioli, F., Wanders, R. J., Aubourg, P., Vianey-Liaud, C., Ijlst, L., Fabre, M., . . . Bougneres, P. F. (1990). Deficiency of long-chain 3-hydroxyacyl-CoA dehydrogenase: A cause of lethal myopathy and cardiomyopathy in early childhood. *Pediatric Research*, *28*, 657-662.
45. Roe, C. R., & Brunengraber, H. (2015). Anaplerotic treatment of long-chain fat oxidation disorders with triheptanoin: Review of 15 years experience. *Molecular Genetics and Metabolism Journal*, *116*, 260-268.

46. Rudolf, M., Rudolf, & Curcio, C. A. (2009). Esterified cholesterol is highly localized to bruch's membrane, as revealed by lipid histochemistry in whole mounts of human choroid. *The Journal of Histochemistry and Cytochemistry*, *57*(8), 731-740. doi:10.1369/jhc.2009.953448
47. Ruitenbeek, W., Poels, P. J., Turnbull, D. M., Garavaglia, B., Chalmers, R. A., Taylor, R. W., & Gabreëls, F. J. (1995). Rhabdomyolysis and acute encephalopathy in late onset medium chain acyl-CoA dehydrogenase deficiency. *Journal of Neurology, Neurosurgery, and Psychiatry*, *58*, 209-214.
48. Saraste, A. (1999). Morphologic criteria and detection of apoptosis. *Cancer Research*, *195*(24), 189-195. doi:10.1007/BF03044961 DO
49. Schrijver-Wieling, I., van Rens, G., Wittebol-Post, D., Smeitink, J., de Jager, J., de Klerk, H., & van Lith, G. R. (1997). Retinal dystrophy in long chain 3-hydroxy-acyl-CoA dehydrogenase deficiency. *British Journal of Ophthalmology*, *81*, 294-294.
50. Schuck, P. F., Ferreira Gda, C., Tahara, E. B., Klamt, F., Kowaltowski, A. J., & Wajner, M. (2010). Cis-4-decenoic acid provokes mitochondrial bioenergetic dysfunction in rat brain. *Life Sciences*, *87*, 139-146.
51. Schuck, P. F., Ferreira Gda, C., Tonin, A. M., Viegas, C. M., Busanello, E. N., Moura, A. P., . . . Wajner, M. (2009). Evidence that the major metabolites accumulating in medium-chain acyl-CoA dehydrogenase deficiency disturb mitochondrial energy homeostasis in rat brain. *Brain Research*, *1296*, 117-126.

52. Schuck, P. F., Ferreira, G. C., Moura, A. P., Busanello, E. N., Tonin, A. M., Dutra-Filho, C. S., & Wajner, M. (2009). Medium-chain fatty acids accumulating in MCAD deficiency elicit lipid and protein oxidative damage and decrease non-enzymatic antioxidant defenses in rat brain. *Neurochemistry International*, *54*, 519-525.
53. Solary, E., Bertrand, R., Kohn, K., & Pommier, Y. (1993). Differential induction of apoptosis in undifferentiated and differentiated HL-60 cells by DNA topoisomerase I and II inhibitors. *Blood*, *81*, 1359-1368.
54. Spiekerkoetter, U. (2007). Effects of a fat load and exercise on asymptomatic VLCAD deficiency. *J Inherit Metab Dis*, *40*, 5.
55. Spiekerkoetter, U., Bastin, J., Gillingham, M., Morris, A., Wijburg, F., & Wilcken, B. (2010). Current issues regarding treatment of mitochondrial fatty acid oxidation disorders. *Journal of Inherited Metabolic Disease*, *33*, 355-361.
56. Spiekerkoetter, U., & Wood, P. A. (2010). Mitochondrial fatty acid oxidation disorders: Pathophysiological studies in mouse models. *Journal of Inherited Metabolic Disease*, *33*, 539-546.
57. Spiekerkoetter, U., Lindner, M., Santer, R., Grotzke, M., Baumgartner, M. R., Boehles, H., . . . Wendel, U. (2009). Management and outcome in 75 individuals with longchain fatty acid oxidation defects: Results from a workshop. *Journal of Inherited Metabolic Disease*, *32*, 488-497.
58. Tait, S., & Green, D. (2012). Mitochondria and cell signalling. *J Cell Sci*, *125*(4), 807-815. doi:10.1242/jcs.099234

59. Tivadar O., Palczewska G., Palczewski K. (2011 May 12). Retinyl ester storage particles (retinosomes) from the retinal pigmented epithelium resemble lipid droplets in other tissues. *J Biol Chem*, 286 (19), 17248-17258.
60. Touma, E. H., & Charpentier, C. (1992). Medium chain acyl-CoA dehydrogenase deficiency. *Archives of Disease in Childhood*, 67, 142-145.
61. Trauner, D. A., Nyhan, W. L., & Sweetman, L. (1975). Short-chain organic acidemia and reye's syndrome. *Neurology*, 25, 296-298.
62. Treem, W. R., Shoup, M. E., Hale, D. E., Bennett, M. J., Rinaldo, P., Millington, D. S., . . . Hyams, J. S. (1996). Acute fatty liver of pregnancy, hemolysis, elevated liver enzymes, and low platelets syndrome, and long chain 3-hydroxyacyl- coenzyme A dehydrogenase deficiency. *American Journal of Gastroenterol*, 91, 2293-2300.
63. Tyni, T., Immonen, T., Lindahl, P., Majander, A., & Kivela, T. (2012). Refined staging for chorioretinopathy in long-chain 3-hydroxyacyl coenzyme A dehydrogenase deficiency. *Ophthalmic Research*, 48, 75-81.
64. Tyni, T., Paetau, A., Strauss, A., Middleton, B., & Kivela, T. (2004). Mitochondrial fatty acid beta-oxidation in the human eye and brain: Implications for the retinopathy of long-chain 3- hydroxyacyl-CoA dehydrogenase deficiency. *Pediatric Research*, 56, 744-750.
65. Tyni, T., Kivela, T., Lappi, M., Summanen, P., Nikoskelainen, E., & P., H. (1998). Ophthalmologic findings in long-chain 3-hydroxyacyl-CoA dehydrogenase deficiency caused by the G1528C mutation: A new type of hereditary metabolic chorioretinopathy . *Ophthalmology*, 105, :810-824.

66. Van Den, B. D., Cubizolle, A., Chatelain, G., Davoust, N., Girard, V., Johansen, S., . . . Mollereau, B. (2018). Physiological and pathological roles of FATP-mediated lipid droplets in drosophila and mice retina. *PLoS Genetics*, *1007627* doi:doi.org/10.1371/journal.pgen.1007627
67. Vockley, J., Burton, B., Berry, G. T., Longo, N., Phillips, J., Sanchez-Valle, A., . . . Kakkis, E. (2017). UX007 for the treatment of long chain-fatty acid oxidation disorders: Safety and efficacy in children and adults following 24 weeks of treatment. *Molecular Genetics and Metabolism*, *120*, 370-377.
68. Waisbren, S. E., Landau, Y., Wilson, J., & Vockley, J. (2013). Neuropsychological outcomes in fatty acid oxidation disorders: 85 cases detected by newborn screening. *Developmental Disabilities Research Reviews*, *17*, 260-268.
69. Wajner, M., & Umpierrez, A. A. (2016). Mitochondrial dysfunction in fatty acid oxidation disorders: Insights from human and animal studies. *Bioscience Report*, *36*, 1-13.
70. Wakabayashi, M., Kamijo, Y., Nakajima, T., Tanaka, N., Sugiyama, E., Yangyang, T., . . . Aoyama, T. (2012). Fatty acid accumulation and resulting PPARalpha activation in fibroblasts due to trifunctional protein deficiency. *PPAR Research*, , 1-7. doi:10.1155/2012/371691
71. Wilcken, B. (2010). Fatty acid oxidation disorders: Outcome and long-term prognosis. *Journal of Inherited Metabolic Disease*, *33*, 501-506.
72. Wilcken, B., Haas, M., Joy, P., Wiley, V., Chaplin, M., Black, C., . . . Boneh, A. (2007). Outcome of neonatal screening for medium-chain acyl-CoA

- dehydrogenase deficiency in australia: A cohort study. *The Lancet*, 369, 37-42.
73. Yang, C., Lim, W., Bazer, W., & Song, G. (2018). Down-regulation of stearoyl-CoA desaturase-1 increases susceptibility to palmitic-acid-induced lipotoxicity in human trophoblast cells. *J Nutr Biochem*, 54, 35-47.
74. Yang, H., Miyahara, H., & Hatanaka, A. (2011). POA and insulin, chronic administration of palmitoleic acid reduces insulin resistance and hepatic lipid accumulation in KK-ay mice with genetic type 2 diabetes zhi. *10(120)*, 1-8. doi:10.1186/1476-511X-10-120.
75. Yang, Z. H., Miyahara, H., & Hatanaka, A. (2011). Chronic administration of palmitoleic acid reduces insulin resistance and hepatic lipid accumulation in KK-ay mice with genetic type 2 diabetes. *Lipids in Health and Disease*, 10(120), 1-8. doi:10.1186/1476-511X-10-120